

**High Performance
Photon Counting**

User Manual

PML-16-C

16 Channel Detector Head for
Time-Correlated
Single Photon Counting

Becker & Hickl GmbH





Becker & Hickl GmbH
High Performance
Photon Counting

March 2006

Tel. +49 / 30 / 787 56 32
FAX +49 / 30 / 787 57 34
<http://www.becker-hickl.de>
email: info@becker-hickl.de

PML-16-C

16 Channel Detector Head for Time-Correlated Single Photon Counting

User Handbook

Simultaneous detection in all 16 channels

Works with all bh TCSPC modules

Routing electronics and high voltage power supply included

Gain control and overload shutdown via bh DCC-100 detector controller card

1-by-16 arrangement of detector channels

IRF width 150 ps FWHM

Count rate up to 4 MHz



Contents

Introduction.....	3
Principles of Multidetector TCSPC.....	4
Operating the PML-16C	7
System Components and Cable Connections	7
Status LEDs	8
TCSPC Parameters	8
System Parameters.....	8
Trace and Display Parameters	9
DCC-100 Parameters.....	12
Internal Discriminator Threshold of the PML-16C	13
Safety	13
Technical Details of Single-Photon Detection	14
Amplitude Jitter of the Single-Photon Pulses.....	14
Constant Fraction Triggering.....	16
Adjusting the CFD Zero-Cross Level.....	17
Adjusting the Discriminator Threshold	17
Channel Uniformity	19
Efficiency.....	19
Transit Time	20
Spectral Response.....	20
Background Count Rate.....	21
Dark Count Rate	21
Afterpulsing	22
PML-SPEC Assembly	24
MW-FLIM Multi-Wavelength FLIM Detection Systems.....	26
One-Photon Excitation with Confocal Detection	26
Two-photon Excitation with Descanned Detection.....	26
Two-photon Excitation with Non-Descanned Detection.....	27
Applications.....	30
Single-point tissue spectroscopy.....	30
Chlorophyll Transients	30
Two-photon Laser Scanning Microscopy of Tissue	32
Troubleshooting.....	34
Assistance through bh.....	35
Specification	36
Electrical	36
Mechanical.....	37
References.....	38
Index	39

Introduction

The PML-16C detector is part of the Becker & Hickl modular multidimensional TCSPC systems. The PML-16-C detects photons simultaneously in 16 channels of a multi-anode PMT. The module connects directly to the bh SPC-130, 140, 150, 630, 730, or 830 TCSPC devices. Signal recording is based on bh's proprietary multi-dimensional TCSPC technique [2, 3, 10]. For each photon the internal routing electronics generate a timing pulse and a detector channel signal. These signals are used in the TCSPC device to build up the photon distribution over the arrival time of the photons and the detector channel number. The result is a set of 16 waveform recordings for the 16 channels of the multi-anode PMT.

The required routing electronics and a high-voltage power supply for the multi-anode PMT is included in the PML-16-C module. The PML-16-C is controlled via the bh DCC-100 detector controller [12]. The DCC-100 provides for the power supply, gain control, and overload shutdown of the PML-16C.

Compared to sequential recording of 16 signals with a single detector the PML-16-C yields a dramatically increased detection efficiency. Typical applications are optical tomography, multi-wavelength fluorescence lifetime microscopy, stopped flow experiments, and classic multi-wavelength fluorescence lifetime experiments. The PML-16 is part of the bh PML-SPEC spectral detection system and the bh multi-wavelength FLIM systems [3].

This handbook covers the general function of the PML-16C, the interaction with the SPC module, the setting of the TCSPC system parameters, and the special technical issues of photon detection with multichannel PMTs. It describes the PML-SPEC spectral detection and MW-FLIM multi-wavelength FLIM detection systems and demonstrates the application of these systems to spectroscopy and imaging of biomedical systems. The basics of multi-dimensional TCSPC are described only briefly. For a comprehensive review of this technique please refer to [2]. For detailed description of the bh SPC modules, the associated SPCM software, applications of the bh TCSPC technique please refer to the bh TCSPC Handbook [3], available on www.becker-hickl.com.

Principles of Multidetector TCSPC

Classic time-correlated single photon counting (TCSPC) is based on the detection of single photons of a periodic light signal, the measurement of the detection times within the signal period, and the reconstruction of the optical waveform from the individual time measurements [26]. Advanced TCSPC techniques are multi-dimensional. They measure not only the times of the photons after the excitation pulses but also the wavelength, the location of emission in a sample, or the times from the start of the experiment [2, 3]. All TCSPC techniques make use of the fact that for low-level, high-repetition rate signals the light intensity is usually low enough that the probability to detect more than one photon per signal period is negligible. Under this condition only one photon per signal period has considered. The photon is detected, its parameters, i.e. time, wavelength, location, etc., are measured, and the distribution of the photon density over these parameters is build up.

Compared with other time-resolved detection techniques TCSPC has a number of advantages, such as superior time resolution, near-ideal (or ‘shot-noise’ limited) sensitivity and signal-to-noise ratio, superior stability of the instrument response function [2, 3, 7], and multi-dimensionality. It is often objected against TCSPC that the count rate must be low enough to make the detection of several photons per signal period unlikely. Often a limit of 0.01 photons per signal period is given for TCSPC [26], but a detection rate up to 0.1 or even 0.2 per signal period can usually be tolerated [2, 3]. Thus, with modern excitation sources count rates on the order of $10 \cdot 10^6 \text{ s}^{-1}$ can be obtained. Acquisition times at such count rates are in the millisecond range.

It is difficult to obtain count rates above $1 \cdot 10^6 \text{ s}^{-1}$ high from biological samples without causing photobleaching or photodamage [6]. In other words, at typical count rates a single TCSPC module with a single detector delivers undistorted waveforms.

Now consider an array of PMT channels over which the same photons flux is spread. Because it is unlikely that the complete array detects several photons per signal period it is also unlikely that several channels of the array will detect a photon in one signal period. This is the basic idea behind multi-detector TCSPC. Although several detectors are *active simultaneously they are unlikely to detect a photon in the same signal period*. The photon pulses delivered by the detectors are therefore unlikely to overlap, and the times of the photons detected in all detectors can be measured in a single TCSPC channel [2, 3, 9].

A block diagram of the PML-16-C is shown in Fig. 1.

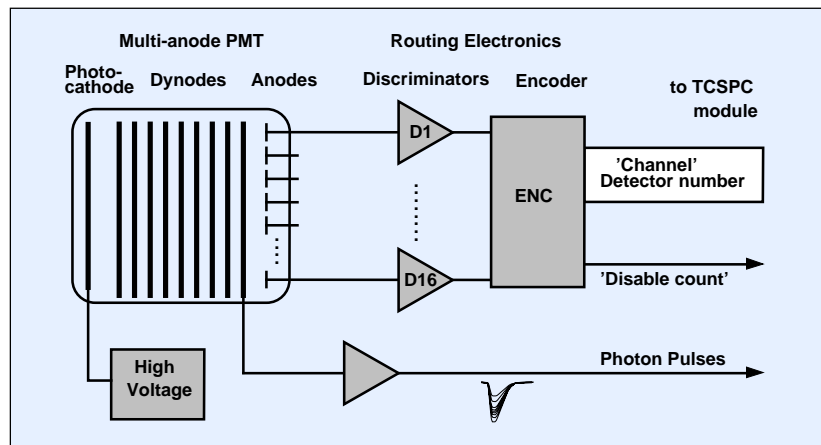


Fig. 1: Block diagram of the PML-16-C

The core of the PML-16 is a Hamamatsu R5900 16 channel multi-anode photomultiplier tube with 16 separate output (anode) elements and a common cathode and dynode system [20, 22]. The photon pulses from the individual anodes are fed into 16 discriminators, D1 through D16. When a photon is detected in any place of the photocathode the corresponding anode delivers a pulse which is detected by one of the discriminators. The discriminator output lines are connected to a digital encoder, ENC. The encoder delivers four ‘channel’ bits and one ‘disable count’ bit. The ‘channel’ bits represent the detector channel which detected the corresponding photon. The ‘disable count’ bit is active when the encoding electronics was unable to provide a valid ‘channel’ data word. This may happen if several PMT channels detected photons simultaneously, or if the current single-photon pulse had an amplitude too small to be detected by the discriminators.

The single-photon pulses of the photons of all detector channels are derived from the last dynode of the R5900 PMT. The output from the dynode is positive. The pulses are amplified and inverted in a wide band amplifier, AMP. The single-photon pulses delivered by the amplifier are compatible with the CFD inputs of the bh TCSPC modules.

Fig. 2 shows how the PML-16C works in concert with the TCSPC module [3]. The CFD of the TCSPC module receives the single-photon pulse from the PML-16C, i.e. the amplified pulse of the PMT channel that detected the photon. When the CFD of the TCSPC module detects this pulse, it starts a normal time-measurement sequence for the detected photon. The time is measured from the photon to the next reference pulse at the stop input of the TCSPC module. This ‘reversed start-stop’ timing allows the TCSPC module to be operated at extremely high pulse repetition rates [3].

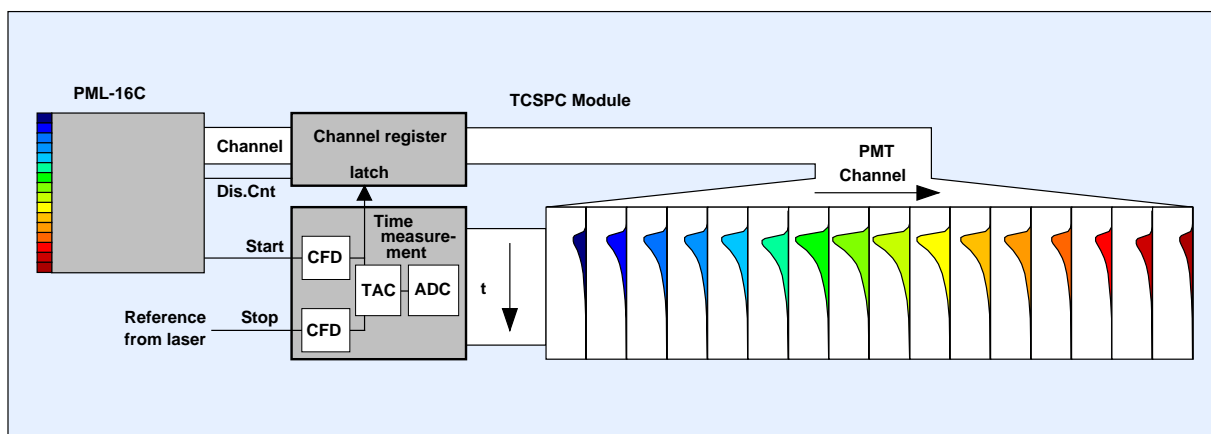


Fig. 2: TCSPC multidetector operation. The TCSPC module builds up the photon distribution over the time in the pulse period and the PMT channel number. The result is 16 separate waveforms for the 16 PMT channels.

The output pulse of the CFD loads the ‘channel’ information from the PML-16C into the channel register of the TCSPC module. The channel information is used as an additional dimension of the recording process. In other words, it controls the memory block in which the photon is stored. Thus, in the TCSPC memory separate photon distributions for the individual detectors build up. In the simplest case, these photon distributions are single waveforms, as indicated in Fig. 2. The technique is often called ‘routing’, because the ‘channel’ data word routes the photons into different waveform blocks of the TCSPC memory.

In the more general case, the TCSPC module may add additional dimensions to the photon distribution recorded. These dimensions may come from the sequencer of the TCSPC board, from the scanning interface, or from additional bits fed into the channel register, see Fig. 3. The TCSPC module builds up a photon distribution over the time, t , in the pulse period, the

detector channel number, the time from the start of the experiment, T , the coordinates of a scanning area, X and Y , and over the information provided by an additional channel data word used to multiplex several lasers or sample positions. Please see [3] for details.

Due to the high count rates applicable with the bh SPC modules there is a non-zero probability to detect more than one photon within the response time of the amplifier/comparator circuitry in the PML-16C. Furthermore, it may happen that the CFD of the SPC detects a photon pulse which was too small to be detected by the PML routing circuitry. In such cases the 'disable count' bit suppresses the recording of the misrouted event in the TCSPC module.

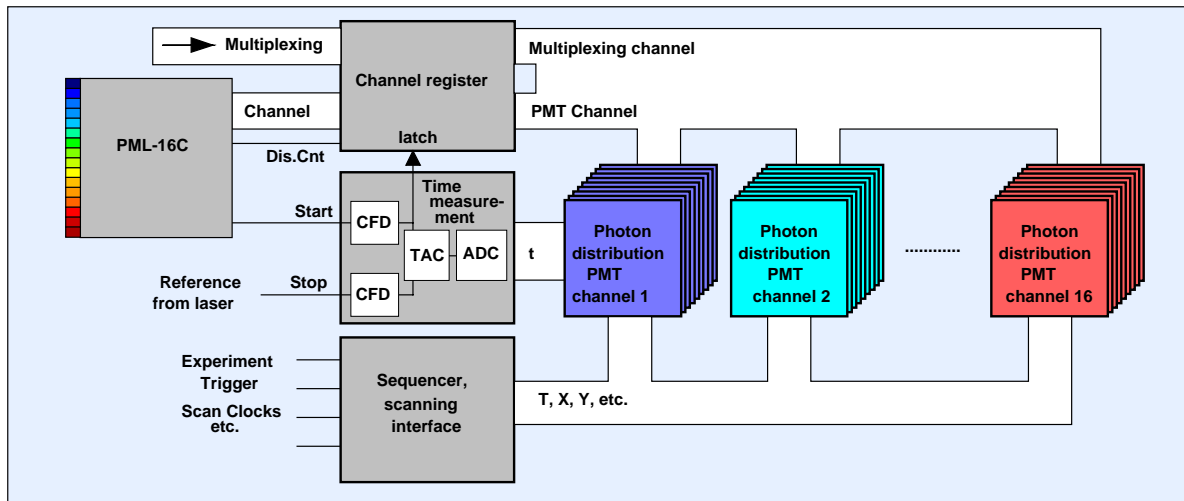


Fig. 3: Multidetector operation of a multi-dimensional TCSPC system. The TCSPC module builds up a photon distribution over the time in the pulse period, the detector channel number, the time from the start of the experiment, the coordinates of a scanning area, and over the information provided by an additional channel data word.

Interestingly, multi-channel detection reduces classic pile-up effects. If several photons arrive within one signal period they are likely to hit the detector in different channels. The 'disable count' bit then suppresses the recording of both photons thus avoiding signal distortion by the loss of only the second photon [2, 3].

Operating the PML-16C

System Components and Cable Connections

The system components and cable connections for operating a PML-16C in a TCSPC system are shown in Fig. 4. The 15 pin sub-D connector of the PML-16C is connected both to the TCSPC module [3] and the DCC-100 detector controller [12]. The TCSPC module can be any of the bh SPC-630, 730, 830, 140/144 or 150/154 modules.

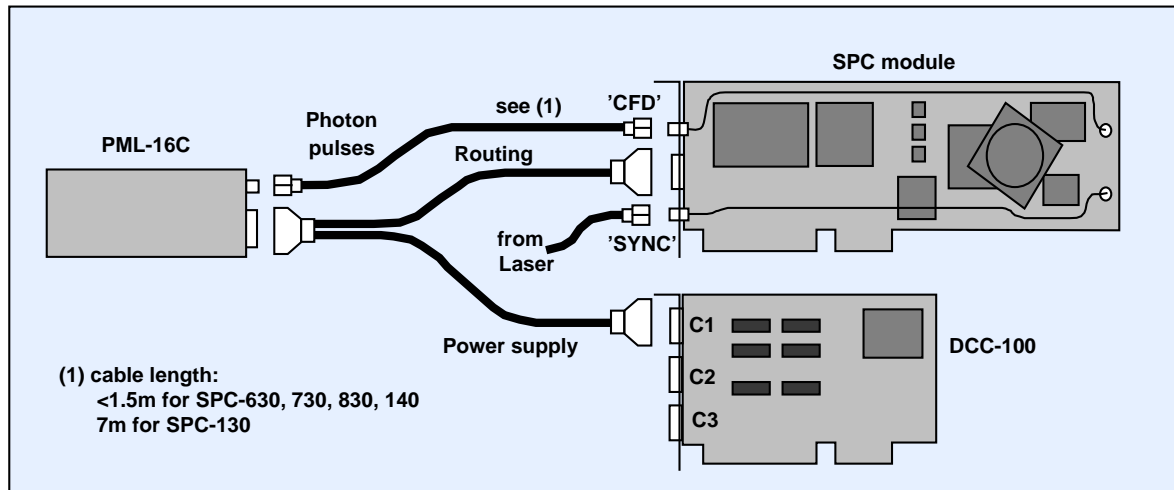


Fig. 4: Cable connections between the PML-16C, the DCC-100 and the TCSPC module.

The routing signals (the 'channel' bits) are connected to the routing input connector of the SPC module. For modules with two connectors (such as the SPC-830) the routing connector is the lower one, i.e. the one closer to the motherboard of the computer. The photon pulses of the PML-16C are connected to the 'CFD' input of the SPC modules. A 50-Ω SMA cable is used for this connection. Except for the SPC-130/134 the photon pulse cable should not be longer than the routing cable in order to maintain correct sampling of the routing bits by the channel register of the SPC module.

The bh SPC-130 modules and the SPC-134 packages were originally designed for multiplexing, not for multi-detector operation. Therefore the SPC-130 cards do not have an adjustable latch delay to read the routing signals from a multichannel detector head. Nevertheless, SPC-130 modules manufactured later than January 2004 can be used with the PML-16C. To provide for the correct latch delay the photon pulses from the PML must be delayed by about 35 ns. This can be achieved by using a 7 m cable in the photon pulse line from the PML to the SPC-130, see Fig. 4.

The older SPC-330, 430, 530 work with the PML-16C in the same way as the SPC-630, 730 and 830. However, these modules have an ISA connector. Because a DCC-100 card is used to control the PML-16C operation with the older SPC modules requires a computer that has both ISA and PCI slots.

Unlike its predecessor, the PML-16 [13], the PML-16C does not require any external high-voltage power supply. The high voltage for the PMT tube is generated internally. The voltage, i.e. the PMT gain, is controlled via a DCC-100 detector controller card. The DCC-100 also delivers the +5V, -5V, and +12V power supply to the PML-16. The PML-16C can be connected both to 'Connector 1' and to 'Connector 3' of the DCC-100.

If the maximum output current of the PMT is exceeded the DCC-100 automatically shuts down the high voltage. This overload protection mechanism normally prevents the PMT from being destroyed. Nevertheless, overload shutdown should be considered an emergency and not be used to switch off the detector in standard situations.

Status LEDs

The PML-16C has three LEDs at its rear panel, see Fig. 5. The 'Count' LED indicates that photons (or at least dark counts) are detected. The 'Count Disable' LED indicates the fraction of photons suppressed by the 'count disable' signal. Please note that there are always some photons that cannot be unambiguously assigned to a particular channel, e.g. photons with extremely small SER amplitudes. The 'overload' LED turns on if the count rate is high so that an increasing number of photons are either rejected or misrouted. It does *not* necessarily mean that the PMT is overloaded. Unless you need maximum routing efficiency you may therefore ignore the overload LED.

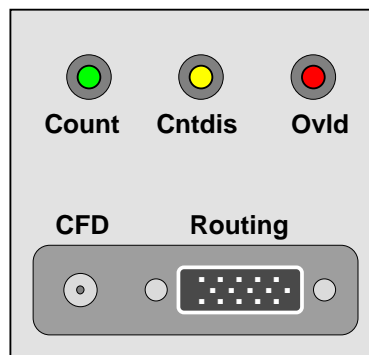


Fig. 5: Rear panel of the PML-16C

TCSPC Parameters

System Parameters

The PML-16C can be used in almost any operation mode of the bh TCSPC modules. To configure the SPC on-board memory for the correct number of data blocks the number of routing channels must be set to '16'. The parameter is defined in the 'Page Control' section of the SPC System Parameters, see Fig. 6.

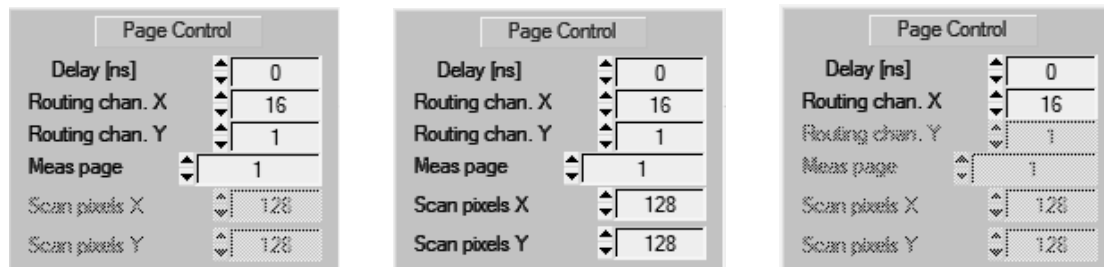


Fig. 6: Defining the number of detector channels in the 'Page Control' section of the SPC system parameters. Left: Single, Oscilloscope, $f(t,T)$ $f(t, ext)$, $fi(t)$, $fi(ext)$ and Continuous Flow mode. Middle: Scan Sync In and Scan Sync Out mode. Right: FIFO (Time-Tag) mode

Except for the SPC-130/134 the 'Page Control' section also contains a 'delay' parameter that is used to define the time after a photon pulse at which the 'channel' data word (i.e. the

routing information) is read into the channel register of the SPC card. The required ‘Delay’ depends on the type of the SPC module:

Module Type	Default Delay	Typical range of Delay for correct operation
SPC-630	0 ns	0 to 10 ns
SPC-730	0 ns	0 to 10 ns
SPC-830	0 ns	0 to 10 ns
SPC-130/134	no ‘Delay’ Parameter, use 7 m CFD cable	-
SPC-140/144	20 ns	0 to 40 ns
SPC-150/154	20 ns	0 to 40 ns

Please make sure that ‘Delay’ is within the range of correct operation. If the routing signals are sampled with a wrong delay the ‘count enable’ signal is not valid, resulting in almost total loss of the detected photons.

As any other PMT, the PML-16C has to be operated with reasonable CFD (constant fraction discriminator) settings. For all SPC-x30 modules we recommend to start with CFD limit low = -80 mV and CFD zero cross = -5 mV. The CFD parameters are accessible either via the ‘System Parameters’ or directly in the main panel of the SPCM software, see Fig. 7. For optimisation of the CFD parameters please see ‘Constant Fraction Triggering’, page 16.

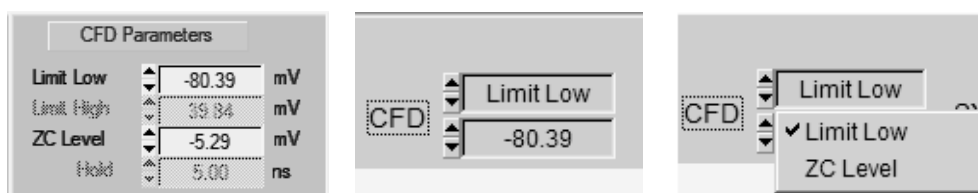


Fig. 7: CFD Parameters. The parameters are accessible via the ‘System Parameters’ (left) or directly in the main window of the SPCM software. (Parameters shown for SPC-x30 modules)

Trace and Display Parameters

With the correct Page Control parameters (Fig. 6) the TCSPC module automatically records 16 separate waveforms for the individual channels of the PML-16C. Depending on the operation mode used the data can be interpreted differently. In the ‘Single’ or ‘Oscilloscope’ mode the data are considered waveforms (usually fluorescence decay curves) at different wavelength or different location at the sample. In the sequential modes the data represent sequences of decay curves at different wavelength or sample position, in the imaging modes images at different wavelengths. Consequently, the bh SPCM software provides different ways to display the data. Details are described in [3]; some examples are shown below.

A typical way to display PML-16C data in the ‘Single’ or ‘Oscilloscope mode’ is shown in Fig. 8. Individual curves are displayed for the individual detector channels. Up to 8 curves can be displayed simultaneously. The curves are defined in the ‘Trace Parameters’, shown in the insert of Fig. 8. The detector channel number is defined by ‘Curve’. By clicking into the ‘Colour’ field for each curve a separate colour can be defined. The display of each curve can be activated and de-activated by clicking on the ‘Active’ button. The SPCM software provides several ‘Pages’ that may contain different measurements or subsequent steps of a sequential measurement. The corresponding data sets are selected by ‘Page’.

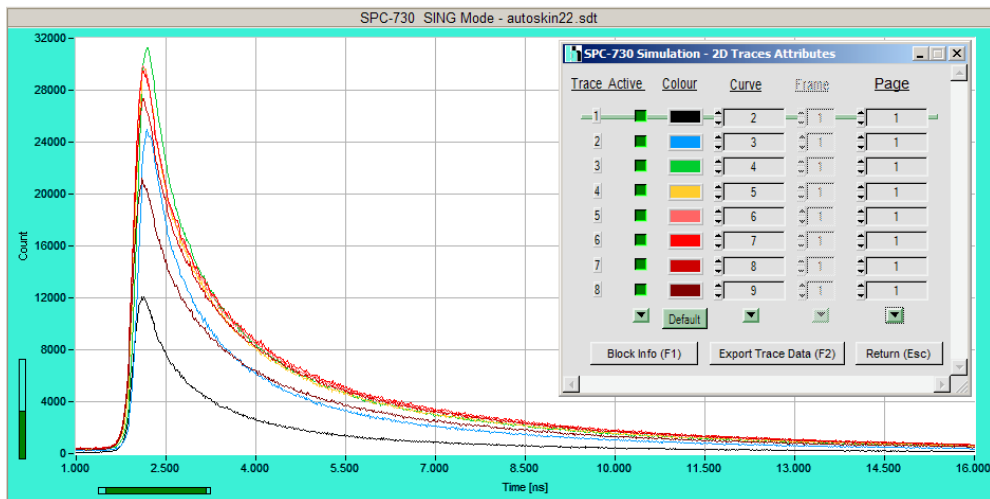


Fig. 8: Display of PML-16C data in the ‘Single’ or ‘Oscilloscope’ mode. Individual curves are displayed for the individual detector channels. The curves are defined in the ‘Display’ parameters of the SPCM software (see insert).

The display of PML-16C data in the $f(txy)$ mode is shown in Fig. 9 and Fig. 10. The figures show autofluorescence data measured at human skin. The fluorescence was detected by a PML-SPEC assembly, i.e. a polychromator was used in front of the PML-16C (see page 24). The data is considered a two-dimensional photon distribution over the time in the fluorescence decay and the wavelength.

The display style is controlled by the ‘Display Parameters’ of the SPCM software, see Fig. 9, right and Fig. 10, right. The display scale can be linear or logarithmic; the display range can be set by an autoscale function or by the operator. Different measurement data sets kept in the memory of the SPC module can be selected by ‘Page’. The Display Parameters provide different display modes (3D curves, Colour-Intensity, OGL Plot). For Fig. 9 the ‘3D curves’ mode was selected for Fig. 10, the Colour-Intensity mode.

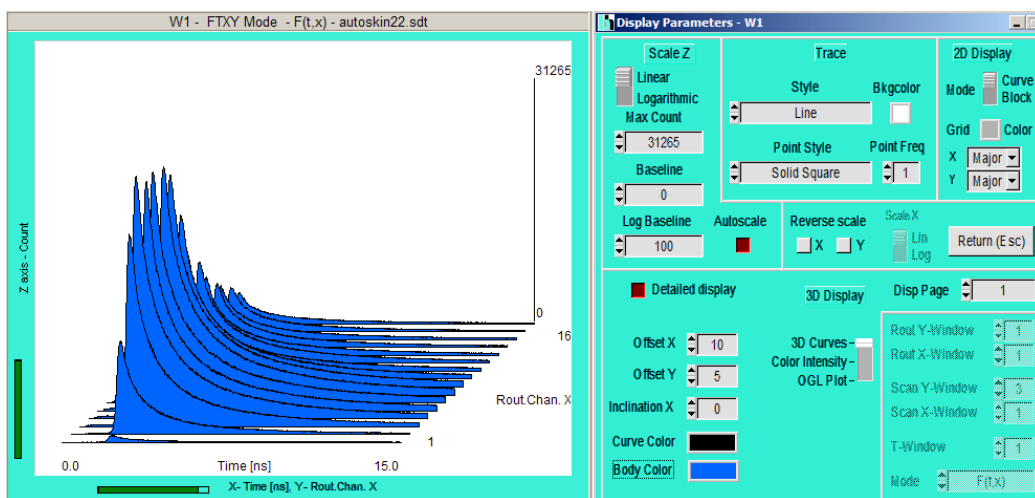


Fig. 9: Display of PML-16C data in the $f(txy)$ mode. The data are shown as a two-dimensional photon distribution over the time within a fluorescence decay and the channel number of the PML-16C. The display is controlled by the ‘Display parameters (right)’. ‘Curve’ mode and linear intensity scale selected. Autofluorescence of skin recorded by PML-SPEC assembly, the channel number represents the wavelength.

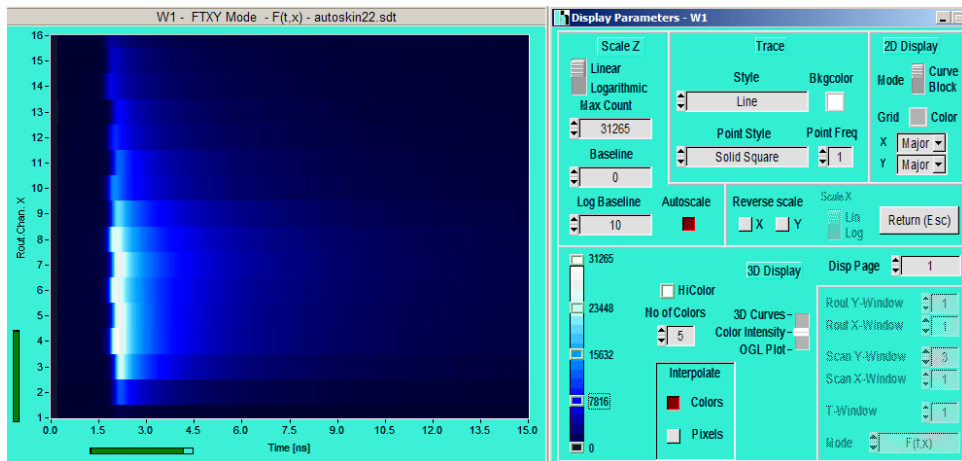


Fig. 10: Display of PML-16C data in the $f(t,x)$ mode. The data are shown as a three-dimensional photon distribution over the time within a fluorescence decay and the channel number of the PML-16C. The display is controlled by the ‘Display parameters (right)’. ‘Colour-Intensity’ mode and linear intensity scale selected. Autofluorescence of skin recorded by PML-SPEC assembly. The channel number represents the wavelength.

Please note that the data structures in the ‘Single’, ‘Oscilloscope’, and ‘ $f(t,x,y)$ ’ modes are identical. Therefore you may run a measurement in the ‘Single’ mode and display the data in the ‘ $f(t, x, y)$ ’ mode or vice versa.

An example of a ‘Scan Sync In’ mode measurement is shown in Fig. 11. The images were taken in a Zeiss LSM 510 NLO two-photon laser scanning microscope upgraded with a bh SPC-830 TCSPC module and a bh MW-FLIM assembly. The sample was an unstained mouse kidney section. Eight display windows were defined showing the integral fluorescence of the sample in eight wavelength intervals. Each image has its own display parameters. The parameters of the left image of the second row are shown right.

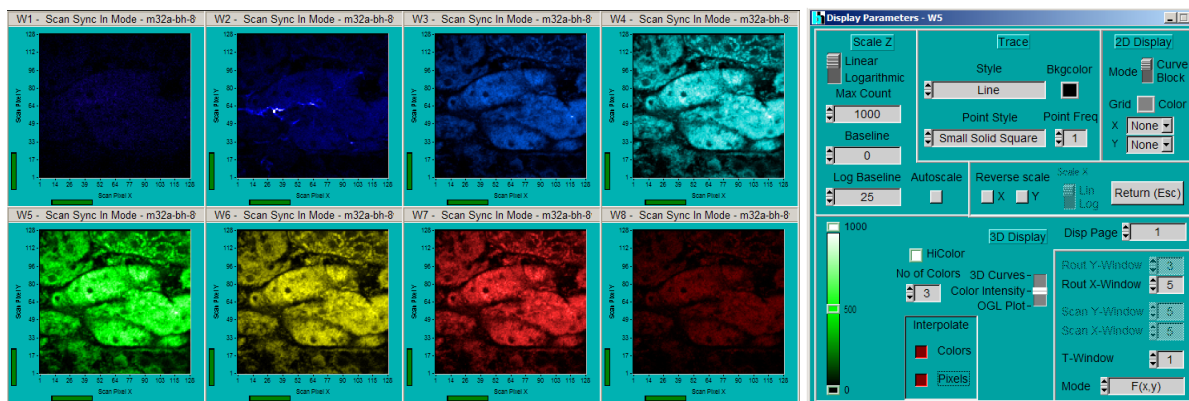


Fig. 11: Multi-wavelength measurement in the ‘Scan Sync In’ mode. LSM 510 two-photon laser scanning microscope, SPC-830 TCSPC module, bh MW-FLIM assembly. The sample is a mouse kidney section. Images in different wavelength intervals are shown left. Each image has its own display parameters; the parameters of the left image of the second row are shown right.

The display mode is the ‘Colour Intensity’ mode. The colours are defined in the lower left of the display parameter panel. They were selected according to the true colour of the wavelength intervals. The wavelength intervals themselves are defined in the ‘Window Parameters’ of the SPCM software (not shown here). The defined wavelength intervals are assigned to the current image by ‘Routing X Window’, in the lower right of the display parameter panel. Images can also be displayed in time-windows specified in the ‘Window Parameters’. The window for the current image is selected under ‘T Window’, in the lower right of the panel.

For details of the display functions please see [3]; for fluorescence lifetime analysis of the images please see [15].

DCC-100 Parameters

The DCC-100 has its own control software [12]. The DCC-100 software is included in the TCSPC installation package, see [3], in TCSPC Handbook, ‘Software Installation’. It can be added to an existing TCSPC installation at any time. The DCC-100 software panel is shown in Fig. 12. The DCC-100 panel can be placed anywhere in the screen area. To keep the panel visible at any time we recommend to switch on the ‘always on top’ function in the ‘Parameters’ of the DCC-100.

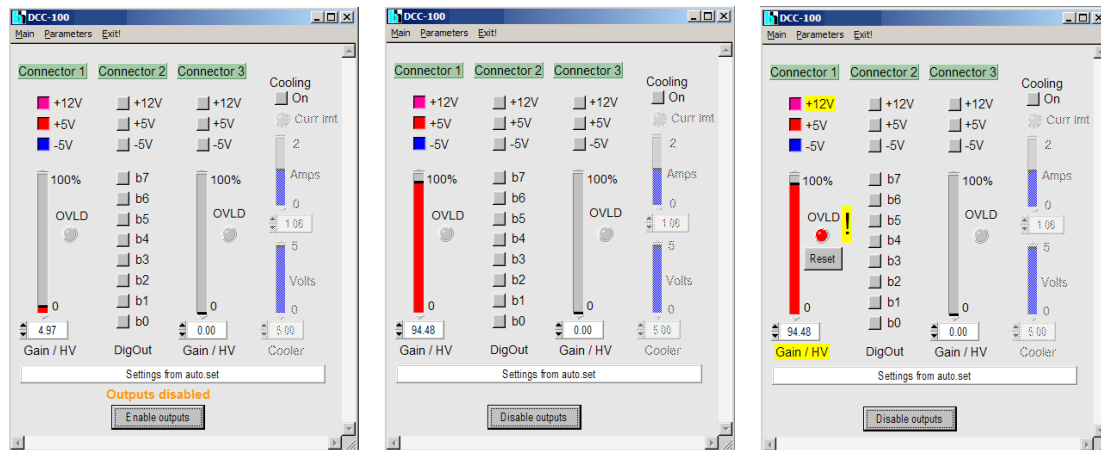


Fig. 12: DCC-100 control panel. Left: After starting the DCC software. Middle: After enabling the outputs. Right: After an overload shutdown.

After starting the DCC-100 software the panel comes up with ‘Outputs disabled’, see Fig. 12, left. This is a safety feature to avoid unintentionally switching on a detector or a high voltage power supply unit that may be connected to the DCC. (The DCC-100 can be configured to start with the outputs enabled, but this configuration should *not* be used for controlling PMTs or any other detectors that use external or internal high voltage.)

The DCC-100 is able to control two detectors, several shutters or actuators, and the thermoelectric coolers of one or two detector modules. The DCC-100 module has three connectors: Connector 1 and connector 3 are for the detectors, connector 2 is for the shutters. The PML-16C can be operated both at connector 1 and at connector 3. For both connectors the control panel contains a ‘Gain’ slider and three buttons for activating the supply voltages. The settings shown in Fig. 12 are for operation of the PML-16C at connector 1.

To operate the PML-16C the supply voltages, +12 V, +5 V, and -5 V, at the used connector must be activated (click on the corresponding buttons). There is no special switch-on sequence. You can turn the supply voltages on and off at any time.

Before enabling the outputs we recommend to turn down the detector gain by pulling down the ‘Gain’ slider. This precaution avoids running into a possible overload condition at full detector gain. After turning down the gain, enable the outputs by clicking on the ‘Enable Outputs’ button and pull up the ‘Gain’ slider. When the gain approaches 80 to 85% you may see the first photons being detected in the SPC module. Check the CFD count rate of the SPC module while further increasing the gain. If the count rate exceeds $5 \cdot 10^6 \text{ s}^{-1}$ decrease the light intensity at the detector. Full operation of the PML-16C is obtained at a gain of 90% to 100%.

The 'Gain' slider controls the *operating voltage* of the PMT. The actual *gain* of a PMT increases with approximately the 4th power of the operating voltage.

Please note:

Photon counting records the pulses the detector delivers for the individual photons of the light signal. The detector gain determines the amplitude of these pulses, not their frequency. The detector gain can therefore *not* be used to control the magnitude of the recorded photon distributions. Any attempt to decrease the sensitivity by reducing the detector gain results in decreased signal-to-noise ratio and poor channel uniformity (see 'Technical Details of Single-Photon Detection', page 14).

If the light intensity at the PML-16C is too high the DCC-100 shuts down the gain and the +12 V supply voltage. In extreme cases this may happen at a gain far below the single-photon detection level, i.e. before the SPC module displays a CFD count rate. The DCC-100 panel after an overload shutdown is shown in Fig. 12, right. If an overload shutdown has occurred, remove the source of the overload. Then click on the 'Reset' button. After the reset the PML-16 resumes normal operation. Please do *not* attempt to avoid overload by operating the PML-16C at reduced detector gain. This would result in poor counting efficiency and poor channel uniformity, see Fig. 21.

Internal Discriminator Threshold of the PML-16C

The PML-16C has 16 internal discriminators to generate the routing information (see Fig. 1, page 4). The threshold of these discriminators can be adjusted by a trimpot. The internal threshold is factory adjusted. *Changing the threshold is not normally needed and therefore discouraged.* If the threshold has been changed for any reasons it can be re-adjusted as described below.

Run a measurement in the oscilloscope mode of the SPC module. Use the stop option 'Stop T' and a collection time of about 1 second. Activate the 'Trace Statistics' panel. Activate the PML-16C but do not send light into the PML-16C. Turn the threshold potentiometer left until the 'Overload' LED at the back of the PML-16C turns on. The threshold is then close to zero. Then turn the potentiometer back (toward higher threshold) until the overload LED turns off.

Send defined light signals to the PML-16C. Adjust the internal threshold in order to obtain a maximum of the 'total counts', good channel separation and good channel uniformity. The final settings may be slightly above, but not far from the point where the overload LED turns off.

Safety

The R5900 PMT of PML-16C is operated at a cathode voltage of up to 1000 V. The cathode voltage is generated by a DC-DC converter inside the PML-16C. Therefore *do not open the housing of the PML-16C when the 15 pin cables from the DCC-100 and the SPC module are connected.* Moreover, please operate the PML-16 only with the correct routing and power supply cables. Make sure that the cables are connected to the correct connectors of the DCC-100 and the SPC module. Using wrong cables or connecting the cables to a wrong connector (e.g. a monitor output from a display card) can seriously damage the PML-16C, the DCC-100, the SPC module or the display card. Make sure not to connect a computer monitor to one of the 15 pin connectors of the DCC-100 of the SPC card. Please do not disconnect any cables when the PML-16C is in operation.

Technical Details of Single-Photon Detection

In early times of TCSPC users were confused by countless and often contradicting instructions about optimising the PMTs of their instruments, configuring constant fraction discriminators, tweaking discriminator thresholds, trigger fractions, and preamplifier bandwidth or gain. The difficulties in part resulted from the slow speed of the early TCSPC electronics and the relatively slow rise times of the single-electron response of the PMTs used. Other advice, such as reducing the relative dark count rate by increasing the CFD threshold, resulted from poorly performing PMTs and preamplifiers or was plainly wrong. Confusion resulted also from applying timing solutions optimised for high-energy particle detection by scintillators straightforward to single-photon detection.

With the currently available high speed constant-fraction discriminators, low-noise preamplifiers, and fast PMTs, adjustments, if required at all, are largely simplified. In fact, all a TCSPC user has to do is to set a discriminator threshold above the noise level of the preamplifier and to increase the operating voltage of the PMT until the counting efficiency starts to saturate.

Nevertheless, the technical details of operating a multichannel PMT in a TCSPC system are described in the following paragraphs. The examples given in this sections are recorded with typical devices. The PMT gain and CFD parameters given are considered representative. Please note, however, that individual PMTs may slightly differ in gain, efficiency, and spectral response.

Amplitude Jitter of the Single-Photon Pulses

A conventional photomultiplier tube (PMT) is a vacuum device which contains a photocathode, a number of dynodes (amplifying stages) and an anode which delivers the output signal [2, 3, 22]. The principle is shown in Fig. 13.

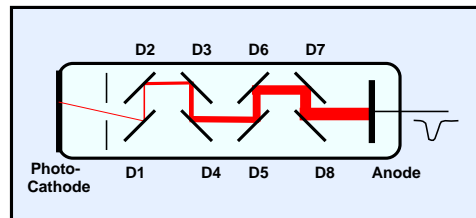


Fig. 13: Principle of a conventional PMT

The operating voltage builds up an electrical field that accelerates the electrons from the photocathode to the first dynode D1, further to the next dynodes, and from D8 to the anode. When a photoelectron hits D1 it releases several secondary electrons. The same happens for the electrons emitted by D1 when they hit D2. The overall gain reaches values of 10^6 to 10^8 . The secondary emission at the dynodes is very fast; therefore the secondary electrons resulting from one photoelectron arrive at the anode within a few ns. Due to the high gain and the short response a single photoelectron yields an easily detectable current pulse at the anode.

The detector output pulse for a single photon, (or a single photoelectron) is called the ‘Single Electron Response’ or ‘SER’. Due to the random nature of the secondary emission, the pulse amplitude varies from pulse to pulse. The secondary emission coefficient at the dynodes is of the order of 5 to 10, resulting in a variation of the number of secondary electrons on the order of 1:2 to 1:4. Moreover, some of the primary electrons are scattered without any multiplication, which further increases the effective width of the amplitude distribution.

The single-photon (SER) pulses of a PML-16C detector are shown in Fig. 14. The pulses have a rise time of about 600 ps and a width of about 2 ns.

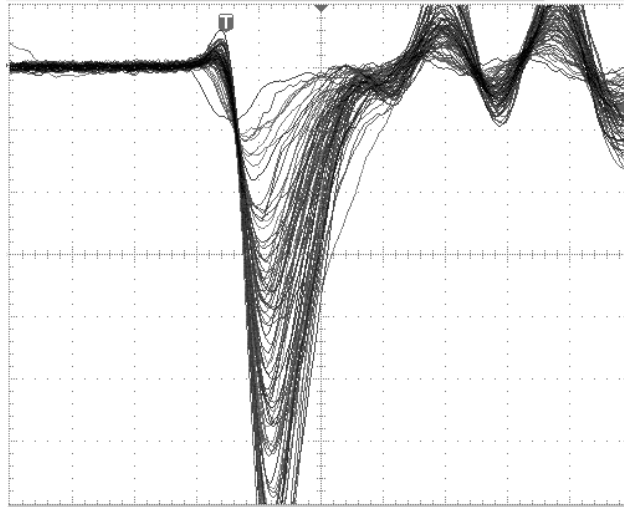


Fig. 14: Single-photon pulses delivered by the PML-16C. Gain = 95%, recorded with Tektronix ??? oscilloscope. Horizontal 2 ns / div, vertical 20 mV / div.

The amplitude of the pulses varies over a wide range. The pulse amplitude distribution measured at three different channels of the same PML-16C is shown in Fig. 15.

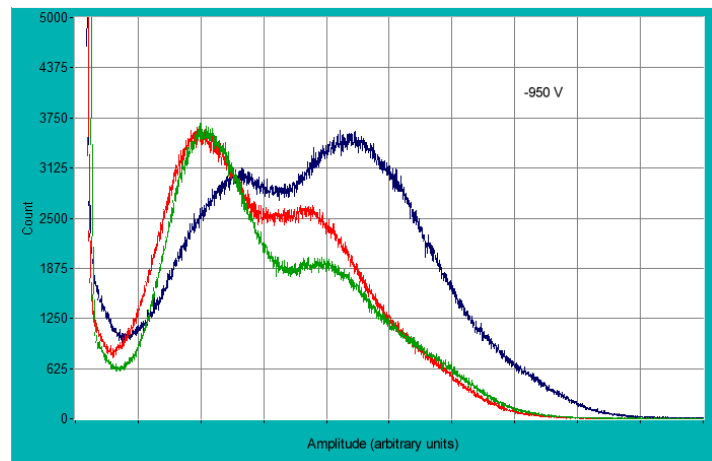


Fig. 15: Amplitude distribution of the single-photon pulses of a PML-16C. Channel 1 (blue), channel 4 (green) and channel 16 (red). DCC gain setting 95%, corresponding to a cathode voltage of -950 V.

Fig. 15 shows that the width at half maximum of the amplitude distribution is 1:3 to 1:4. The pulse amplitude distribution consists of three major components. The largest part of the distribution, above about 1 unit, is due to the regular single-photon pulses. It also contains background pulses due to thermal emission at the photocathode. The amplitude distribution is slightly different for different channels, which has to be taken into regard when the CFD threshold is optimised (see Fig. 21).

Especially at high gain there is usually a sub-structure in the amplitude distribution. It is probably caused by spatial nonuniformity in the secondary emission coefficient, and by the discrete number of secondary electrons emitted at the first dynode.

Thermal emission, photoelectron emission, and reflection of primary electrons at the dynodes cause an increase of the pulse density at low amplitudes. At very low amplitudes electronic

noise, either from the preamplifier or from the environment, causes a third peak of extremely high count rate.

The amplitude jitter of the SER pulses sets two general requirements to the input discriminator circuitry in the TCSPC module. On the one hand, the trigger delay must be independent of the variable amplitude of the pulses. On the other hand, the discriminator threshold must be high enough to reject the electronic noise and the pulses caused by thermal emission in later stages of the dynode chain of the PMT.

Constant Fraction Triggering

In a simple leading-edge trigger the amplitude jitter of the single-photon pulses would introduce a timing jitter on the order of the rise time of the pulses. Therefore ‘Constant Fraction Discriminators’, or ‘CFDs’ are used in the start and stop inputs of the bh TCSPC modules. A CFD virtually triggers at a constant fraction of the peak amplitude of the input pulse. In practice constant fraction triggering is achieved by triggering on the zero cross of the difference of the delayed and the undelayed input pulse [2, 3]. The principle is shown in Fig. 16.

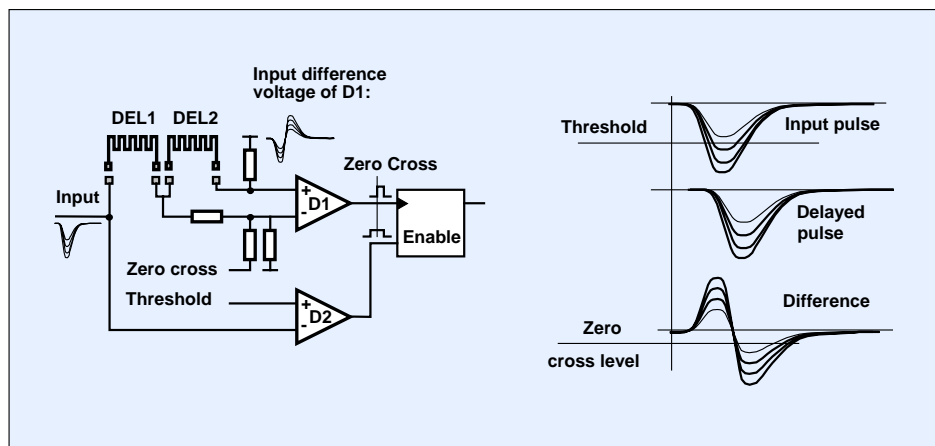


Fig. 16: Principle of the CFDs of the bh TCSPC boards

The CFD contains two fast differential discriminators, D1 and D2. D2 triggers when the input amplitude exceeds a selectable ‘CFD threshold’. After a small delay, DEL1, the same input pulse is fed into the differential inputs of D1. However, the signal at the non-inverting input of D1 is given an additional delay, DEL2. D1 triggers when the difference of the voltages at its inputs crosses the baseline, as shown in Fig. 16, right. A fast D-flip-flop is enabled by the pulse of D2 and triggered by the transition of D1. Thus, the flip-flop is triggered when a zero cross at D1 occurs while the input voltage exceeds the CFD threshold.

Ideally, the temporal location of the zero cross does not depend on the amplitude. The circuit shown in Fig. 16 therefore meets the requirements of single-photon timing: Pulses below a defined amplitude are rejected, and the amplitude jitter has no influence on the timing.

Theoretically minimum timing jitter should be expected at a zero-cross level of exactly zero. However, in practice the zero-cross discriminator has an offset voltage of a few mV. Moreover, the intrinsic delay of the discriminator depends on the amplitude of the input signal. The corresponding contribution of the discriminator to the timing jitter can be compensated for by a ‘CFD Zero-Cross Level’ slightly offset from the signal baseline.

Adjusting the CFD Zero-Cross Level

The dependence of the instrument response function (IRF) of one channel of a PML-16C on the zero-cross level is shown in Fig. 17. Due to the fast discriminators used in the CFDs of the bh TCSPC modules the influence of the zero-cross level on the IRF is small. A reasonable IRF is obtained within a range of +30 mV to -30 mV, best results within +10 mV to -10 mV. The adjustment of the zero cross is therefore not critical, or, in many cases, even not necessary.

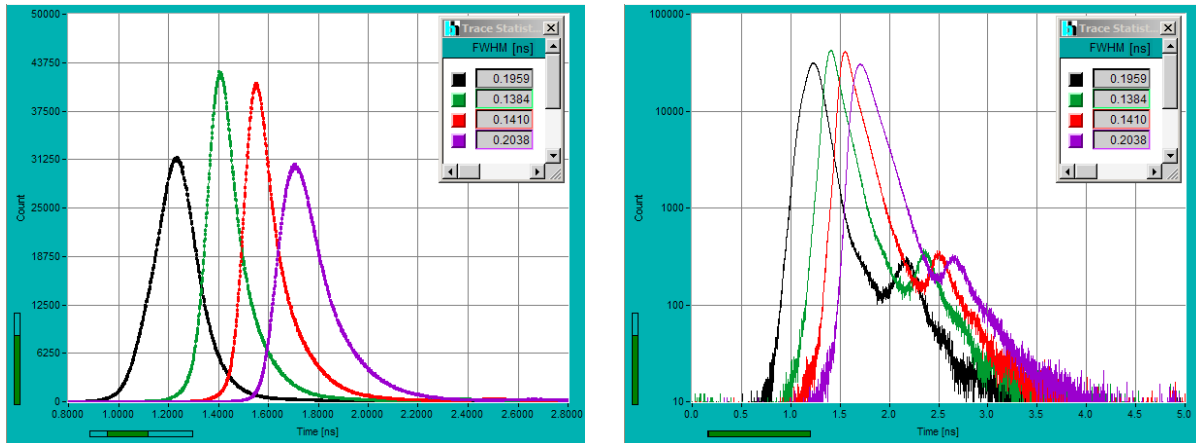


Fig. 17: Dependence of the IRF of a single PML-16C channel on the CFD Zero-Cross Level. Black +30 mV, green +10 mV, red -10 mV, magenta -30 mV. The FWHM of the IRF is shown in the inserts. Left: Linear scale, 200 ps / division, 1.22 ps / point. Right: Logarithmic scale, 500 ps / division, 1.22 ps / point. Light pulses from BHL-600 diode laser, pulse width 30 ps, repetition rate 50 MHz.

Zero-cross levels closer than 5mV to the signal baseline should be avoided. In that case, the zero-cross discriminator may trigger due to spurious signals from the synchronisation channel or may even oscillate. Of course, spurious triggering and oscillation stop when an input pulse arrives, but some after-ringing may still be present and modulate the trigger delay. The result can be poor differential nonlinearity (ripple in the recorded curves) or a double structure in the IRF.

Adjusting the Discriminator Threshold

A TCSPC system should record the regular photon pulses, but not the thermal dynode pulses and the electronic noise background. Therefore, the optimum CFD threshold is near the valley between the regular photon pulse distribution and the peak caused by electronic noise and dynode emission, see Fig. 18, left. The pulse amplitude distribution stretches horizontally with increasing PMT gain. Therefore the optimum CFD threshold increases with the PMT gain.

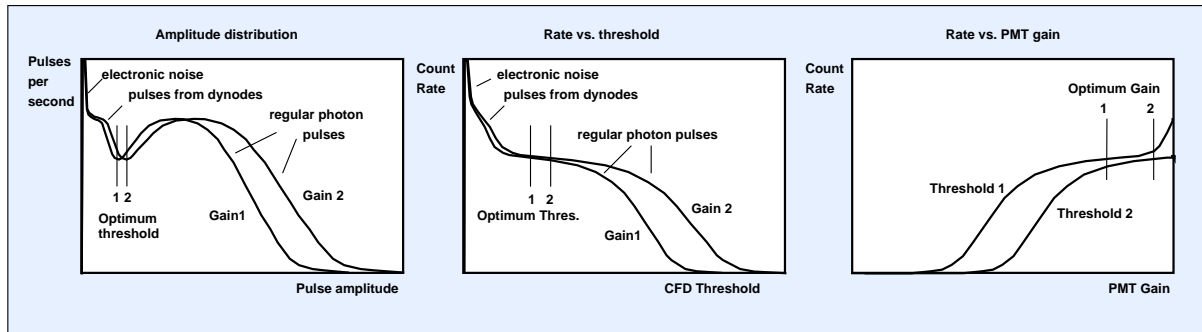


Fig. 18: Left: General shape of the amplitude distribution of the single-photon pulses. Middle: Dependence of the count rate on the CFD threshold. Right: Dependence of the count rate on the PMT gain.

The corresponding dependence of the count rate on the discriminator threshold is shown in Fig. 18, middle. The PMT is illuminated with light of low intensity. When the discriminator threshold ('CFD limit Low') is decreased the count rate increases. At a sufficiently low threshold the increase of the count rate flattens, and in the ideal case forms a plateau. The PML-16C-0 and -1 detectors the counting plateau is clearly visible. For other PMTs the plateau may be not very pronounced. However, at least a flattening of the count rate increase should be found.

At very low threshold the count rate increases again because thermal dynode pulses or electronic noise are detected. In practice the dynode peak may be not very prominent or even be hidden in the electronic noise.

A similar behaviour is found if the gain of the PMT is changed, see Fig. 18, right. The count rate increases with increasing gain and eventually reaches a plateau.

Consequently, there are two ways to find a reasonable operating point of the PMT: You may either set a reasonable PMT gain and vary the CFD threshold, or set a reasonable CFD threshold and vary the PMT gain. For the PML-16C the DCC gain should be between 90 and 95 %, corresponding to a PMT operating voltage between 900 and 950 V. The CFD threshold should be within a range of -50 to -100 mV.

The CFD threshold, does, of course also influence the shape of the IRF. An example is given in Fig. 19. The CFD threshold was increased in 20 mV steps from -20 mV to -140 mV. At very low threshold (-20 mV and -40 mV) the IRF develops a shoulder prior to the mean peak. The shoulder is typical of front-window PMTs operated at low threshold. Most likely, it is caused by photoelectron emission at the first dynode. A clean IRF at good efficiency is obtained for thresholds from -60 mV to -100 mV. The efficiency drops noticeably at -120 mV and -140 mV. Despite of the short IRF width (see inserts in Fig. 19) operating the PML-16C in this threshold range is discouraged. The high threshold not only results in loss of photons but also in large efficiency differences between the channels (see paragraph below).

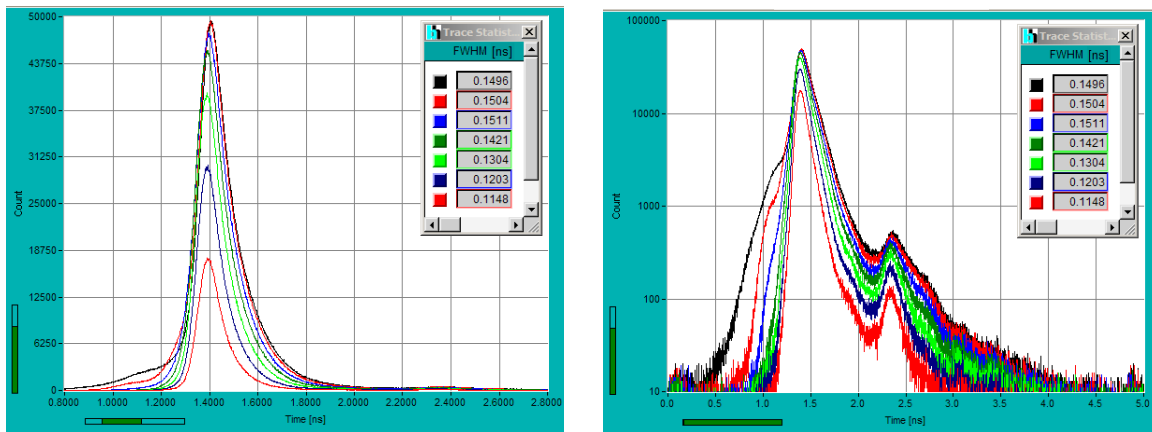


Fig. 19: IRF for CFD thresholds from -20 mV to -140 mV. The FWHM of the IRF is shown in the insert. Left: Linear scale, 200 ps / division, 1.22 ps / point. Right: Logarithmic scale, 500 ps / division, 1.22 ps / point. Light pulses from BHL-600 diode laser, pulse width 30 ps, repetition rate 50 MHz.

Channel Uniformity

Efficiency

For a multichannel PMT the CFD threshold has also a noticeable influence on the uniformity of the channels in terms of efficiency. Although all PMT channels use the same dynode system and the same operating voltage the pulse amplitude distribution for the individual channels may differ noticeably (see Fig. 15). The situation is illustrated in Fig. 20. PMT channel B has a gain 25% lower than channel A. Threshold 2 yields a satisfactory efficiency for channel A, but not for channel B. If this threshold is used the result is a large variation in the efficiency of the channels. Better results are obtained with threshold 1. Both channels are then in the 'counting plateau', and the gain difference has little influence on the efficiency. For the PML-16C it is therefore important to set the PMT gain high enough for the CFD threshold used (or the CFD threshold low enough for the gain used) to obtain reasonable counting efficiency for the channel of the lowest gain.

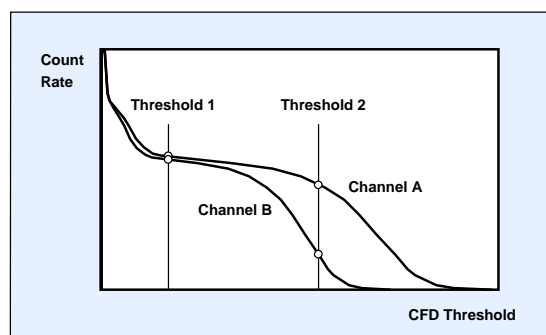


Fig. 20: Effect of gain variations of the PMT channels

A practical example is given in Fig. 21. The channels of a PML-16C were evenly illuminated with continuous light. The DCC gain was set to 95%, corresponding to a PMT operating voltage of 950 V. From left to right, the CFD threshold was increased from -40 mV to -120 mV. It can clearly be seen that with increasing CFD threshold there is not only a decrease in efficiency but also a degradation in the channel uniformity.

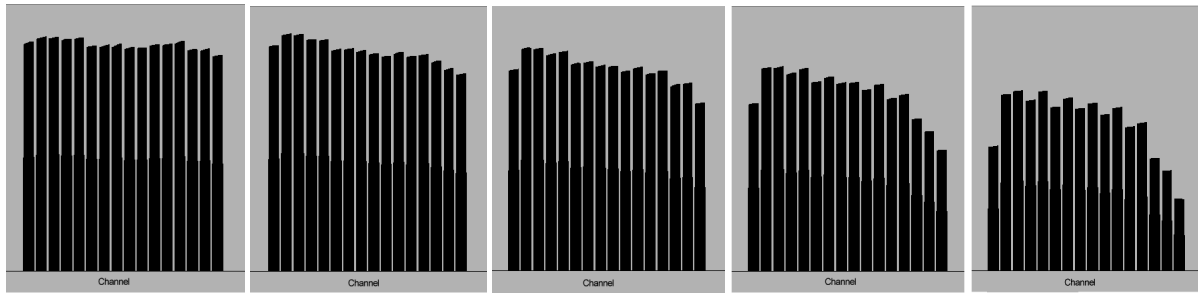


Fig. 21: Uniformity of the efficiency of the PML-16C channels. DCC gain setting 95%. Left to right: CFD threshold -40 mV, -60 mV, -80 mV, -100 mV, -120 mV

Transit Time

Photomultipliers of the metal channel type have a noticeable dependence of the transit time on the location on the photocathode [3]. The R5900 tube used in the PML-16C is no exception. Fig. 22 shows that there is a systematic wobble in the transit time of the channels. The effect has to be taken into account in the data analysis, either by determining individual IRFs for the channels or by including a shift parameter in the fit procedure.

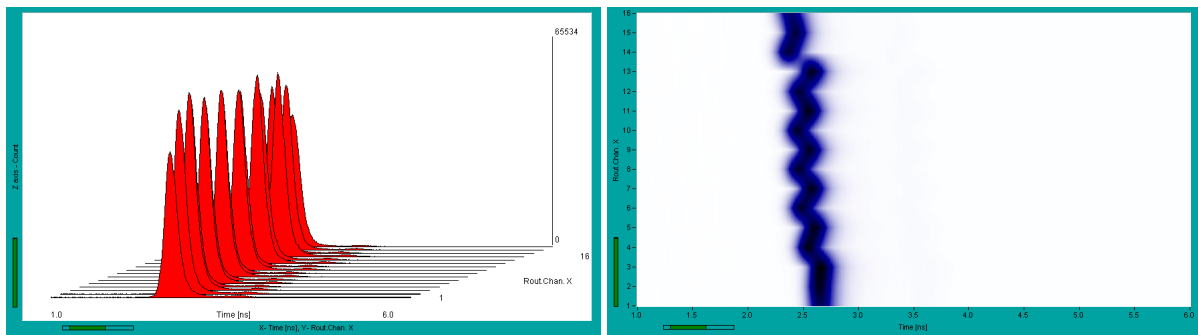


Fig. 22: Instrument response functions of the PML-16C channels. Response to 50 ps diode laser pulses at 650 nm. Left: curve plot. Right colour-intensity plot, vertical axis is the channel number.

Because of the transit time differences we do not recommend to combine PMT channels directly, i.e. by changing the connections of the routing bits. The result would be a loss in time resolution.

Spectral Response

The PML-16C comes in two photocathode versions. The typical spectral response is shown in Fig. 23. The bialkali cathode of the PML-16C-0 has a high efficiency in the blue range of the spectrum and can be used from about 320 nm to 600 nm. The multi-alkali cathode (PML-16C-1) has its efficiency maximum in the green region of the spectrum. It can be used from about 320 nm to 800 nm. Please note that the formation of the photocathode of a PMT is a complicated and in some details empirical process. Even with modern manufacturing techniques results are not accurately predictable. Thus, the spectral sensitivity of individual PMTs may differ slightly in the peak value and in the spectral shape.

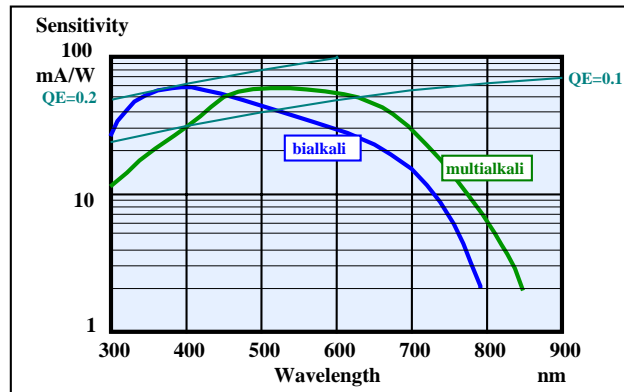


Fig. 23: Typical spectral sensitivity of the bialkali and the multialkali photocathode, after [22].

Spectral sensitivity specifications of PMTs are given in mA photocurrent per Watt incident power. The quantum efficiency, QE , can be calculated from the spectral sensitivity by

$$QE = S \frac{hc}{e\lambda} = \frac{S}{\lambda} \cdot 1.24 \cdot 10^{-6} \frac{\text{Wm}}{\text{A}}$$

with S = Spectral Sensitivity, h = Planck constant, e = elementary charge, λ = Wavelength, c = velocity of light.

Background Count Rate

Dark Count Rate

The dark count rate of a PMT is dominated by thermal electron emission from the photocathode. Consequently, the amplitude distribution of the output pulses is essentially the same as for the photoelectrons. Only at very low amplitudes there is a contribution of thermal emission from the dynodes. With a correctly adjusted CFD threshold these pulses are rejected anyway. Attempts to reduce the dark count rate by further increasing the CFD threshold are therefore useless. The only effect would be a decrease in counting efficiency, i.e. the dark count rate would decrease by the same ratio as the photon count rate. Moreover, the channel uniformity would be impaired, for reasons described above.

The only way to keep the dark count rate low is to reduce the temperature of the detector. A decrease in temperature by 10 °C results in a decrease in the dark count rate by a factor of about 5, depending on the cathode material. Even a small decrease in temperature can therefore have a large effect. At an ambient temperature of 22°C typical total dark count rates for the PML-16C are 20 to 200 for -0 (bialkali) and 400 to 2000 for the -1 (multialkali) versions.

Exposure of the cathode to room light increases the dark count rate temporarily, even if no operating voltage is applied to the PMT. The increase can be as large as a factor of 100. The dark count rate resumes its normal value after some time. Full recovery can take several hours.

Exposure to strong light with the PMT operating voltage being switched on (i.e. with a DCC gain setting >0) can increase the dark count rate permanently. The overload shutdown function of the PML-16C - DCC-100 combination makes this kind of damage unlikely. Nevertheless, extreme overload should be carefully avoided.

Afterpulsing

The dark count rate is often considered the only source of signal background. Signal background can, however, also be caused by afterpulsing. All photon-counting detectors (also single-photon avalanche photodiodes) have an increased probability of producing background pulses within a few microseconds following the detection of a photon. These afterpulses are detectable in almost any conventional PMT. It is believed that they are caused by ion feedback, or, by a smaller amount, by luminescence of the dynode material and the glass of the tube.

Afterpulsing becomes noticeable especially in high-repetition rate TCSPC applications, in particular with Ti:Sapphire lasers or diode lasers. At high repetition rate, the afterpulses from many signal periods pile up and can cause a considerable signal-dependent background. The total afterpulsing rate can easily exceed the dark count rate of the detector by a factor of 100 [2, 3].

The R5900-L16 tubes used in the PML-16C have a relatively low afterpulsing probability and thus deliver an excellent dynamic range in high-repetition rate applications. Fig. 24, upper row, shows a recording of a fluorescence signal, taken with a PML-16C-0 in PML-SPEC multi-spectral detection assembly (see paragraph below).

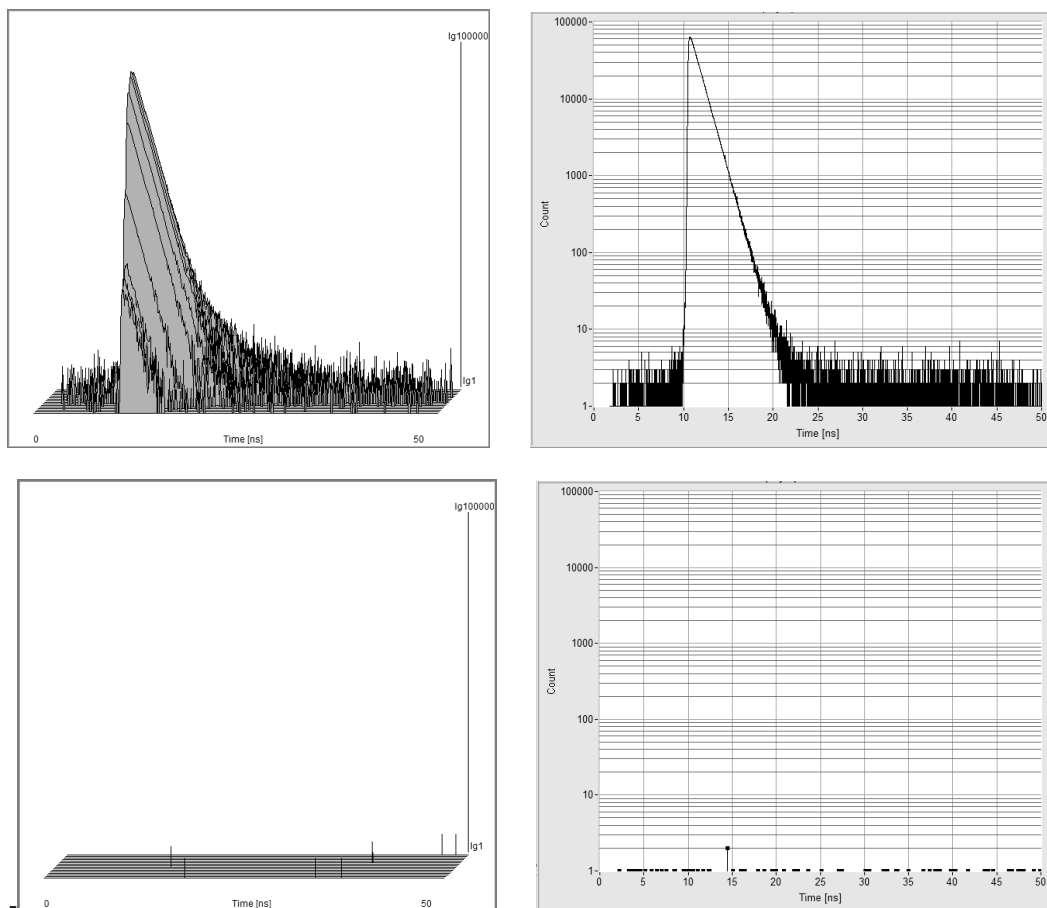


Fig. 24: Background by afterpulsing. Left: Fluorescence signal. Right: Dark counts. Upper row: All 16 wavelength channels. Lower row: Channel with maximum fluorescence intensity. Laser pulse repetition rate 20 MHz, acquisition time 100 seconds.

The acquisition time was 100 seconds. The excitation pulse rate was 20 MHz, the acquisition time 100 seconds. The complete multi-spectral decay data are shown left, the channel of

highest intensity right. The useful dynamic range (peak to background) is more than 4 orders of magnitude, about as good as for an MCP PMT [3].

A dark recording taken with the same acquisition time and pulse repetition rate as the fluorescence recording is shown in the lower row of Fig. 24. It is obvious that the dark count level is lower than the background of the fluorescence recording. The average background levels are 1.8 and 0.015, respectively. Thus, also for the PML-16C the dynamic range at high pulse repetition rate is limited by afterpulsing, not by the dark count rate.

The straightforward way to reduce the afterpulsing background is to reduce the signal repetition rate. However, to keep pile-up effects low the count rate must be reduced [2, 3]. The tradeoff is therefore an increased acquisition time.

PML-SPEC Assembly

The PML-SPEC multi-wavelength detection assembly is a combination of the PML-16C and a small grating polychromator (or spectrograph). The assembly is shown in Fig. 25.

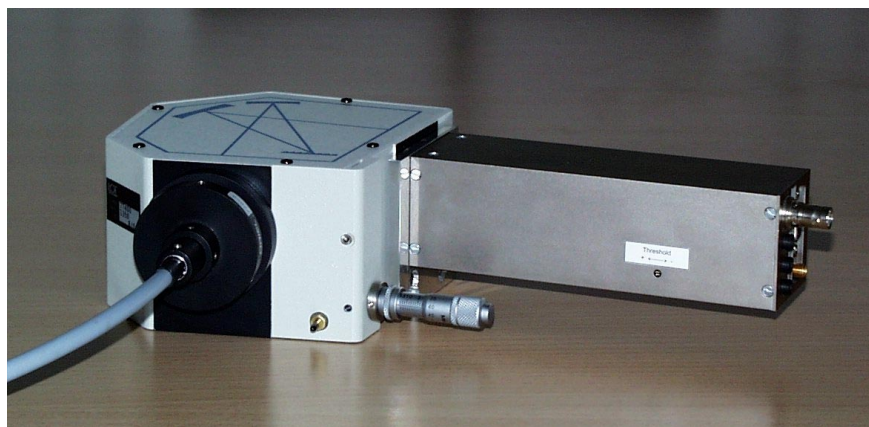


Fig. 25: PML-SPEC multi-wavelength detection assembly, shown with a fibre bundle at the input

The PML-SPEC is available with three different gratings, see table below. The grating determines the dispersion and thus the wavelength interval recorded via the 16 channels of the PML-16C. The start wavelength of the interval is selectable by a micrometer screw at the polychromator.

Grating Part No.	Primary wavelength region adjustable by set screw	Width of recorded wavelength interval, channel 1 to 16	Blaze Wavelength
77417	340-820 nm	300 nm	500 nm
77414 (standard)	340-820 nm	200 nm	400 nm
77411	340-820 nm	100 nm	350 nm

The blaze wavelength is the wavelength the grating is optimised for. The amount of light diffracted into the first diffraction order is at maximum at this wavelength. However, even at a wavelength close to the blaze wavelength a grating disperses some light into higher diffraction orders. The light of the unused orders can cause substantial straylight problems. In fluorescence applications the PML-SPEC should therefore be used with an additional filter that blocks the excitation wavelength.

There are several ways to deliver the light into the input slit plane of the polychromator. Free-beam coupling is often used in the traditional fluorescence lifetime setups. In these cases a lens transfers the luminescent spot in the sample into the input slit of the polychromator. The parameters of this lens have a considerable influence on the optical efficiency.

The polychromator accepts light within a focal ratio (or 'f number') of about 1:3.5. To obtain maximum light throughput, the f number of the input light cone must match the f number of the monochromator. Moreover, the image in the input plane must not be larger than the slit. Building an appropriate relay lens system is no problem if the light comes from a point source. For larger sources the throughput is limited by the slit size and the f number of the monochromator; see Fig. 26.

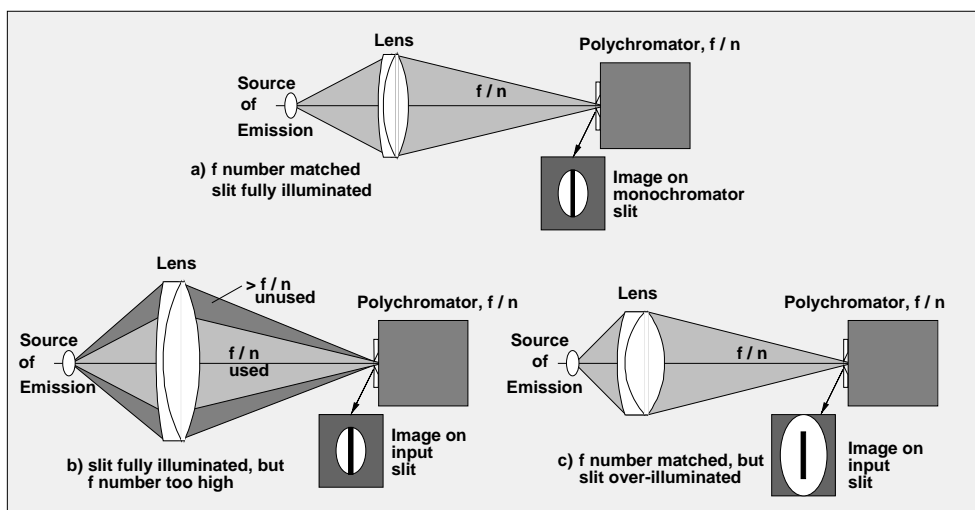


Fig. 26: Limitations of the light throughput of a polychromator. Once the slit is fully illuminated and the f numbers are equal, neither (a) a larger lens nor (b) a lens with a higher NA at the source side will increase the throughput.

Once the input light cone matches the f number of the polychromator (a), neither (b) a larger lens nor (c) a lens with a higher NA at the source side will increase the amount of transmitted light. Case (b) leads to an input cone of a larger f number than accepted by the polychromator. Case (c) results in an image larger than the polychromator slit. In both cases the additional light transferred by the lens is not transmitted through the polychromator.

Please note that relatively wide input slits can be used for the PML-SPEC. The centre distance of the PML-16C channels is 1 mm. Reducing the slit width far below this value does not yield any gain in resolution. Thus, the optimum slit width is in the range of 0.5 to 1 mm.

Another way to increase the throughput is to reduce the size of the excited spot in the sample or to match the shape of the source spot to the monochromator slit. In cuvette fluorescence systems with a horizontal excitation beam a large improvement can be made by turning the polychromator 90°, so that the slit is horizontal and matches the orientation of the excited sample volume.

Another way to couple light into the PML-SPEC is via an optical fibre. For fibre-coupled systems the input slit of the polychromator is replaced with a fibre adapter, with the end of the fibre placed in the slit plane. The coupling efficiency from the fibre into the polychromator is then almost ideal. However, coupling the light into the fibre has to cope with the same basic optical problems as coupling the light directly into the polychromator slit. Fibre diameters up to 1 mm can be used without much compromise in wavelength resolution. Fibre-coupled systems are used to connect the PML-SPEC to confocal scan heads of laser scanning microscopes [8], see Fig. 27. Fibre-coupling has also been used for diffuse optical tomography (DOT). A super-continuum was generated by sending the pulses of a Ti:Sapphire laser through a photonic crystal fibre. After propagating of the continuum pulses through the tissue the light was collected via a multi-mode fibre, and the time-of-flight distributions were recorded in 16 wavelength intervals [1].

An elegant way to increase the throughput of a fibre-coupled system is to use several fibres or a fibre bundle (see Fig. 28 and Fig. 30). The fibres are arranged along the slit of the polychromator. The fibre system is thus used to collect light from an increased area and transform the cross-section of this area into the cross section of the slit.

MW-FLIM Multi-Wavelength FLIM Detection Systems

The PML-SPEC assembly is used for bh's modular fluorescence lifetime imaging (FLIM) systems for laser scanning microscopy [3, 5]. Laser scanning microscopes scan the sample by a focused laser beam and detect the fluorescence from the excited spot by a single-point detector. Confocal microscopes use a pinhole in the detection light path to suppress light from outside the focal plane [27]. Two-photon microscopes excite the fluorescence by a femtosecond laser of high repetition rate. Two photons of the input light are used to generate one fluorescence photon [18, 19]. Two-photon excitation is nonlinear and thus yields noticeable excitation only in the focus of the microscope objective lens. Therefore excitation outside the focal plane is avoided altogether.

One-Photon Excitation with Confocal Detection

The general setup of a confocal multi-wavelength FLIM system is shown in Fig. 27. A bh BDL-405-SM diode laser [14] delivers picosecond pulses into one of the laser input fibres of the scanning microscope. In order to obtain diffraction-limited focusing the laser scanning microscopes use single-mode fibres for the laser input. Therefore the -SM (single-mode) version of the BDL-405 must be used. The power of the laser is controlled via the DCC-100 card.

The fluorescence light from the scanned spot of the sample is fed into the PML-SPEC via a multi-mode fibre output from the scan head. Fibre outputs are available for almost all modern laser scanning microscopes. Diode-laser based confocal MW-FLIM systems are available for the Zeiss LSM 510, the Olympus FV1000, and the Leica SP2 or SP5.

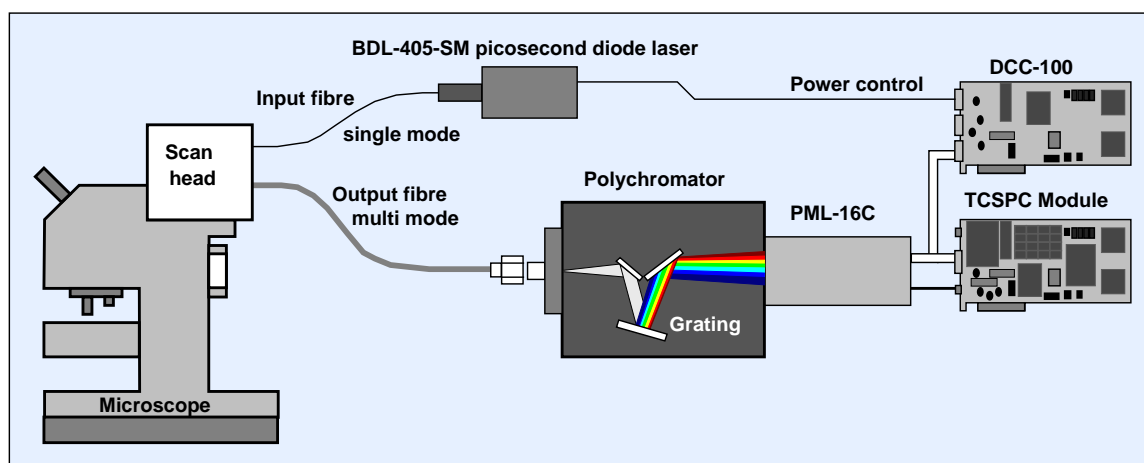


Fig. 27: Multi-wavelength FLIM system, one-photon excitation by picosecond diode laser, confocal detection

The TCSPC module is operated in the 'Scan Sync In' mode. In this mode the recording in the TCSPC module is synchronised with the scanning by pixel clock, line clock, and frame clock pulses from the microscope. The TCSPC module builds up a photon distribution over the time in the laser pulse period, the coordinates of the scan, and the wavelength [2, 3, 5]. Because of the large amount of data to be kept in the TCSPC memory an SPC-830 module should be used.

Two-photon Excitation with Descanned Detection

With a femtosecond Ti:Sapphire laser the sample can be excited by two-photon absorption [18, 19]. In a microscope, two-photon excitation works with high efficiency because the energy density in the focus of a high-NA objective lens is high. Noticeable excitation is

obtained only in the focus. Therefore two-photon excitation inherently delivers depth resolution. Confocal detection through a pinhole is not required. Nevertheless, the fluorescence light can be fed back through the scanner and the pinhole. The optical setup of the detection light path is then identical with the one used for one-photon excitation. System with two-photon excitation and detection via the confocal beam path have been used for FRET experiments [8, 17] and for PDT experiments on the cell level [28].

Two-photon Excitation with Non-Descanned Detection

Because two-photon excitation does not generate fluorescence outside the focus no light from outside the focal plane needs to be rejected. The fluorescence light can therefore be diverted directly behind the microscope objective by a dichroic mirror. This setup is called ‘non-descanned’ or ‘direct’ detection in contrast to the ‘confocal’ or ‘descanned detection’ used for one-photon excitation.

Two-photon excitation in conjunction with non-descanned detection can be used to image tissue layers several 100 μm deep [18, 21]. Since the scattering and the absorption coefficients at the wavelength of the two-photon excitation are small the laser beam penetrates through relatively thick tissue. Even if there is some loss on the way through the tissue it can be compensated by increasing the laser power. Of course, the fluorescence photons are scattered on their way out of the tissue and therefore emerge from a relatively large area of the sample surface. Moreover, the surface is not in the focus of the objective lens. The fluorescence light therefore leaves the full back aperture of the microscope lens in a cone of relatively large angle. A multi-wavelength system for non-descanned detection systems has to transfer this light into the polychromator.

The first multi-spectral FLIM system for two-photon microscopes with non-descanned detection was described in [16]. An image of the aperture of the microscope objective lens was projected on the input of a 1-mm multi-mode fibre. The fibre delivered the fluorescence light to a polychromator. The spectrum was recorded by a bh PML-16 detector, and the 16 wavelength channels were recorded simultaneously by a bh SPC-830 module. The problem of the optical setup used was that a strong demagnification into the fibre has to be used. This results in a high numerical aperture of the light cone at the input of the fibre. However, a multi-mode fibre used near its maximum NA develops strong pulse dispersion [24]. The IRF of the system is therefore noticeably broader than the IRF of the PML-16. Moreover, the short focal length required for the projection into the fibre results in a small diameter of the lens. The system therefore loses efficiency for deep layers of highly scattering samples.

The bh NDD MW-FLIM systems use a fibre bundle to transform the circular cross section of the microscope lens aperture into the linear cross section of the polychromator slit. The principle is shown in Fig. 28.

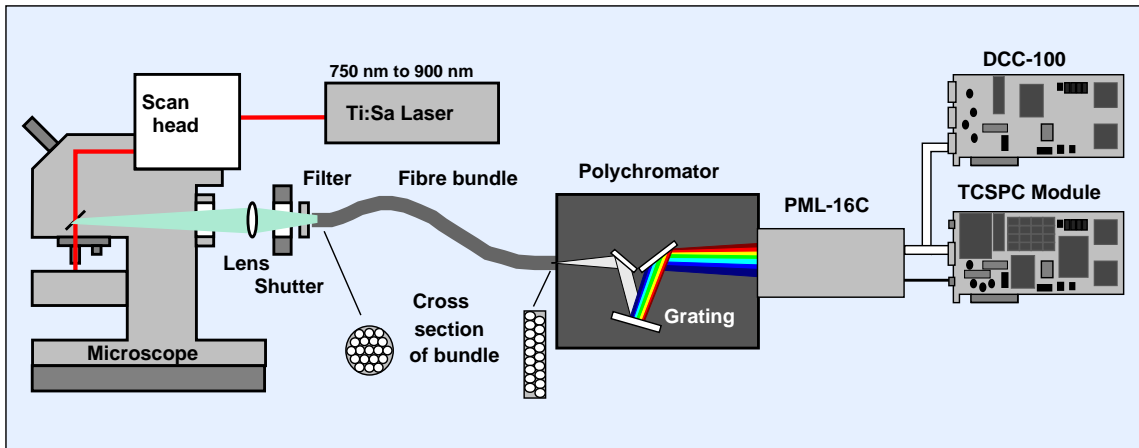


Fig. 28: Multi-wavelength FLIM system, two-photon excitation and non-descanned detection

A field lens projects an image of the effective aperture of the microscope lens on the input of a fibre bundle. The fibre bundle has a circular cross section at the input, and a rectangular cross section at the output. Thus, the input matches the image of the microscope lens aperture. The output matches the input slit of the monochromator. The system features high efficiency even for highly scattering samples. Moreover, the fibre bundle is illuminated at moderate NA so that pulse dispersion is small.

Please note: The input face of the fibre bundle must be placed in a plane *conjugate with the aperture of the microscope lens*. Placing the input face in a plane *conjugate with the sample* results in scanning the luminescent spot over the face of the fibre bundle. The result would be that the structure of the fibre bundle appears in the image. You can find the right plane by turning on the microscope lamp in the transmission light path and checking the image in the plane of the bundle input face. The image is bright enough to show up on a piece of paper.

Due to the large light collection area non-descanned detectors can be severely overloaded by daylight leaking into the detection path. Moreover, the halogen or mercury lamp of the microscope is a potential a source of detector damage. Therefore all bh FLIM systems for non-descanned detection not only use detector overload shutdown but also a shutter to avoid excessive exposure of the photocathode [2, 3, 5, 11]. The field lens is integrated in the shutter assembly.

The essential parts of the bh NDD ME-FIM system are shown in Fig. 29. The shutter assembly is shown left, the fibre bundle in the middle. The PML-SPEC with the adapter for the fibre bundle is shown right.

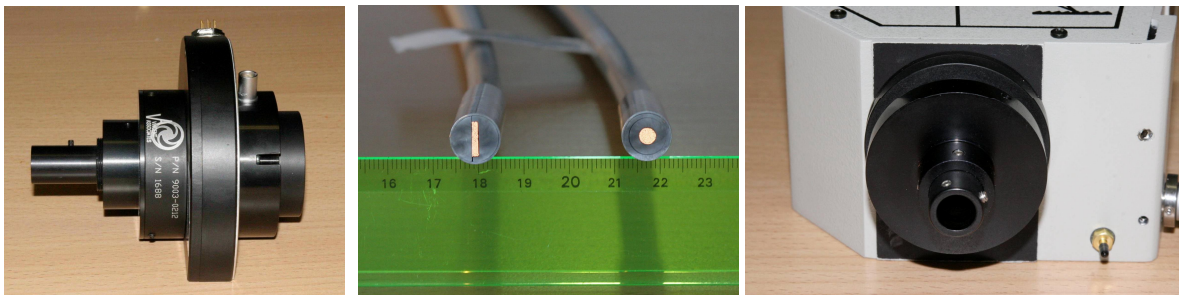


Fig. 29: NDD MW-FLIM system. Left: Shutter assembly with integrated field lens, fibre bundle adapter and adapter to Zeiss LSM-510 NDD switch box. Middle: Fibre bundle. Right: Input side of polychromator with adapter for fibre bundle.

The NDD MW-FLIM systems are available for the Zeiss LSM 510 NLO microscopes and for Leica SP2 and SP5 MP systems. The shutter assembly of the MW-FLIM connects to the NDD switch box of the LSM 510 and to the RLD port of the SP2 or SP5. The assemblies can, however, easily be adapted to non-descanned ports of other microscopes.

Applications

Single-point tissue spectroscopy

An application of the PML-SPEC to single-point autofluorescence measurements of biological tissue is shown in Fig. 30 and Fig. 31. The system consists of a 405 nm or 375nm picosecond diode laser, a fibre probe, the polychromator, the PML-16C, a bh TCSPC module and a DCC-100 card [4].

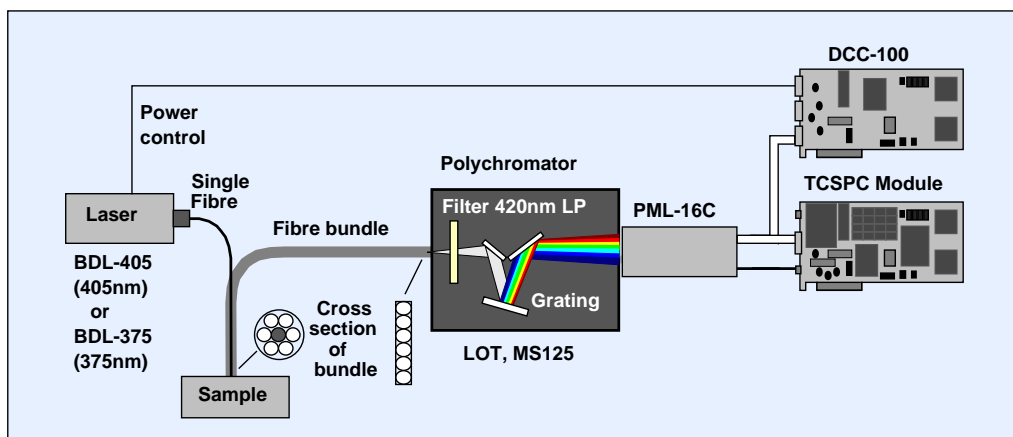


Fig. 30: Single-point multi-wavelength fluorescence lifetime system

Multi-spectral fluorescence decay data of human skin obtained this way are shown in Fig. 31. The sample was excited at 405 nm, at a power of about $60 \mu\text{W}$. The count rate at this power was about $2 \cdot 10^6 \text{ s}^{-1}$. Multi-wavelength decay data of good accuracy are obtained within a few seconds.

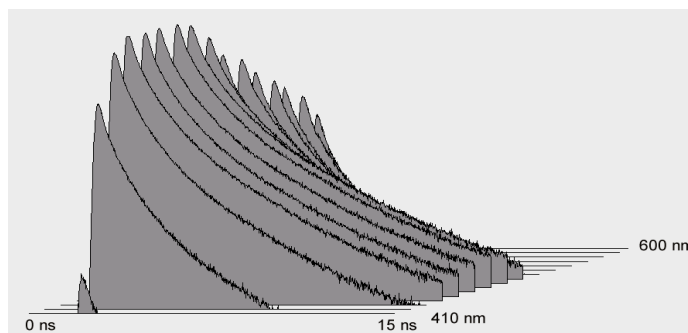


Fig. 31: Autofluorescence of human skin, recorded by the system shown in Fig. 30. 1024 time channels, logarithmic scale from 500 to 30,000 counts per channel, excitation wavelength 405 nm.

Chlorophyll Transients

If sample exposure and acquisition time are not important results like the one shown in Fig. 31 can, in principle, also be obtained by scanning the wavelength by a monochromator and recording the decay curves at different wavelength sequentially. Multi-wavelength detection becomes, however, mandatory if transient fluorescence effects are to be investigated or if a sample is scanned at high pixel rate.

Typical examples of transient fluorescence effects are the ‘fluorescence transients’ of chlorophyll in living plants [25]. When a dark-adapted leaf is exposed to light the intensity of the chlorophyll fluorescence starts to increase. After a steep rise the intensity falls again and

finally reaches a steady-state level. The rise time is of the order of a few milliseconds to a second, the fall time can be from several seconds to minutes. The initial rise of the fluorescence intensity is attributed to the progressive closing of reaction centres in the photosynthesis pathway. Therefore the quenching of the fluorescence by the photosynthesis decreases with the time of illumination, with a corresponding increase of the fluorescence intensity. The fluorescence quenching by the photosynthesis pathway is termed 'photochemical quenching'. The slow decrease of the fluorescence intensity at later times is termed 'non-photochemical quenching'.

Results of a non-photochemical quenching measurement are shown in Fig. 32. The fluorescence in a leaf was excited by a bh BDL-405 (405 nm) picosecond diode laser. Simultaneously with the switch-on of the laser a recording sequence was started in the TCSPC module. 30 recordings were taken in intervals of 2 seconds; Fig. 32 shows four selected steps of this sequence. The decrease of the fluorescence lifetime with the time of exposure is clearly visible.

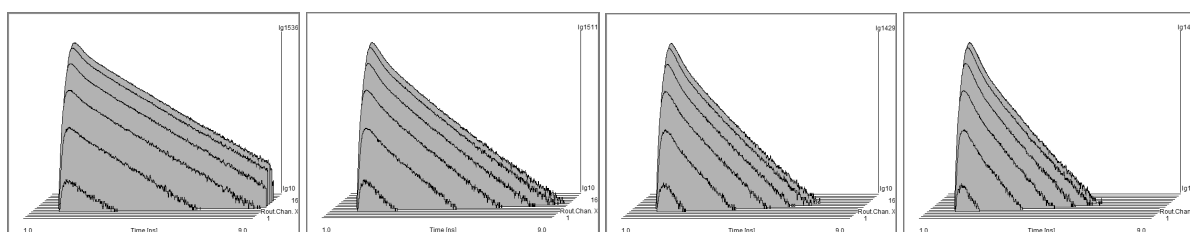


Fig. 32: Non-photochemical quenching of chlorophyll in a leaf, excited at 405 nm. Recorded wavelength range from 620 to 820 nm, time axis 0 to 8 ns, logarithmic display, normalised on peak intensity. Left to right: 0 s, 20 s, 40 s, and 60 s after start of exposure.

Fig. 33 shows fluorescence decay curves at selected wavelengths versus the time of exposure, extracted from the same measurement data set as Fig. 32. The sequence starts at the back and extends over 60 seconds. Also here, the decrease of the fluorescence lifetime with the time of exposure is clearly visible.

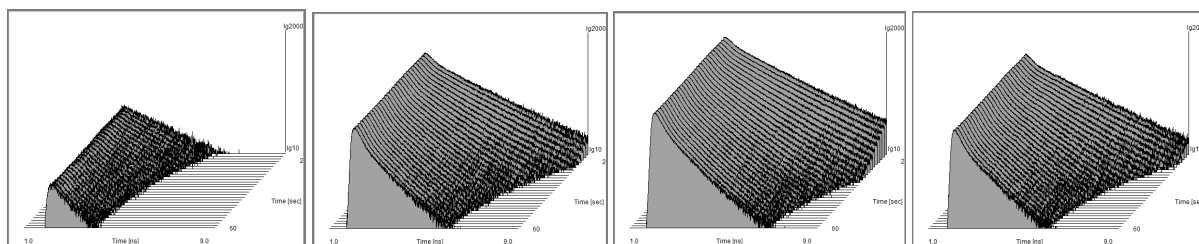


Fig. 33: Non-photochemical quenching of chlorophyll in a leaf, excited at 405 nm. Fluorescence decay curves in different wavelength channels versus time of exposure. 2 s per curve, sequence starts from the back. Extracted from same measurement data as Fig. 32.

The non-photochemical transients shown above occur on a time scale of several 10 seconds. Good results are therefore obtained by recording a single sequence of decay curves at an acquisition time of a few seconds per curve.

The photochemical quenching transients are much faster. Recording these transients requires a resolution of less than 100 μ s per step of the sequence. Of course, the number of photons detected in a time this short is too small to build up a reasonable decay curve. Photochemical quenching transients must therefore be recorded by triggered sequential recording [2, 3]. The principle is shown in Fig. 34. The excitation laser is periodically switched on an off. Each 'on' phase initiates a photochemical quenching transient in the leaf; each 'off' phase lets the leaf

recover. Within each 'on' phase a fast sequence of decay curves is recorded in the TCSPC module. The measurement is continued for a large number of such on-off cycles, and the results are accumulated.

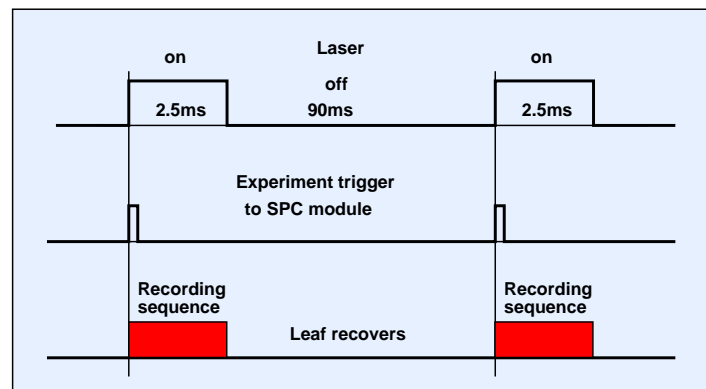


Fig. 34: Triggered sequential recording of photochemical quenching transients. The laser is cycled on and off. Each 'on' phase starts a photochemical quenching transient in the leaf. A sequence of waveform recordings is taken within each 'on' phase. A large number of such on/off cycles is accumulated to obtain enough photons with the individual steps of the accumulated sequence.

A typical result is shown in Fig. 35. The 'on' time was 2.5 ms. Within this time a sequence of 50 decay curves of 50 μ s collection time each was recorded. The 'off' time was 90 ms. 20,000 of such on-off cycles were accumulated.

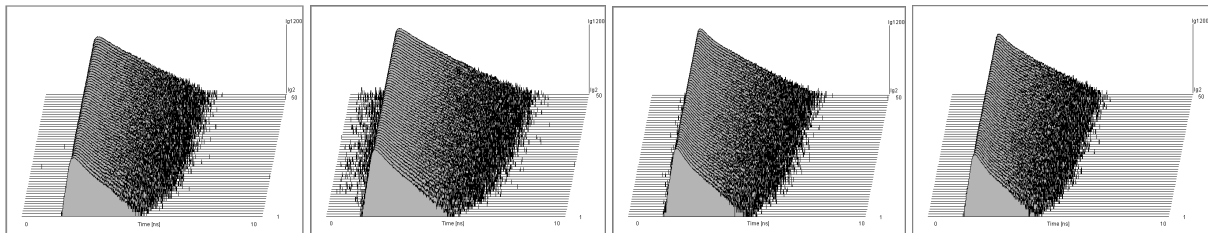


Fig. 35: Photochemical quenching of chlorophyll in a leaf. Fluorescence decay curves in different wavelength channels versus time. Triggered sequential recording, 50 μ s per curve, 20,000 measurement cycles accumulated

Two-photon Laser Scanning Microscopy of Tissue

Fig. 36 and Fig. 37 show autofluorescence images of mouse kidney tissue, obtained in a Zeiss LSM 510 NLO microscope. The fluorescence was excited by two-photon excitation at 750 nm. The MW-FLIM system shown in Fig. 28 was connected to the output of non-descanned detection (NDD) switch box of the LSM 510. The FLIM data were acquired for 10 minutes at a count rate of about 10^5 photons/s. Higher count rates and correspondingly shorter acquisition times are technically possible but cause unacceptable photobleaching in the sample.

Fig. 36 shows lifetime images for the individual wavelength intervals of the PML-SPEC assembly. The colour represents the lifetime of a single-exponential fit applied to the decay data in the pixels. Except for the first two images (which do not contain fluorescence photons) the intensity was normalised to obtain the same brightness for the brightest pixels. Due to the different fluorophores present in the tissue, the lifetimes in the individual wavelength intervals are different. The blue features in the third and fourth images are due to SHG (second harmonic generation) in the tissue. SHG is an extremely fast process and reveals itself as an infinitely short lifetime component.

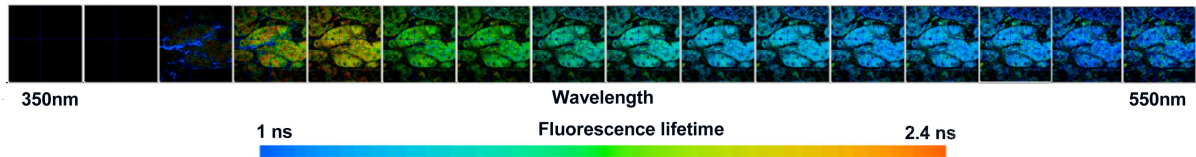


Fig. 36: Autofluorescence FLIM images of living mouse kidney tissue.

An increased signal-to-noise ratio is obtained by combining the decay data of several wavelength intervals, see Fig. 37. The upper row shows single-exponential lifetime images in wavelength intervals of 350 to 380 nm, 380 to 430 nm, 430 to 480 nm, and 480 to 530 nm.

The second row, left, shows the fluorescence decay curve at the cursor position of the 430 to 480 nm image. Even at first glance it can be seen that the decay is not single-exponential. A good fit can be obtained by a double-exponential fit. The lifetime images in the second row show the fast decay component, the slow decay component, and the amplitude ratio of both. The fluorescence in the 430 to 480 nm interval is dominated by NADH. The lifetime of NADH is known to depend on the binding to proteins [23]. The images can therefore be expected to represent different binding states of NADH.

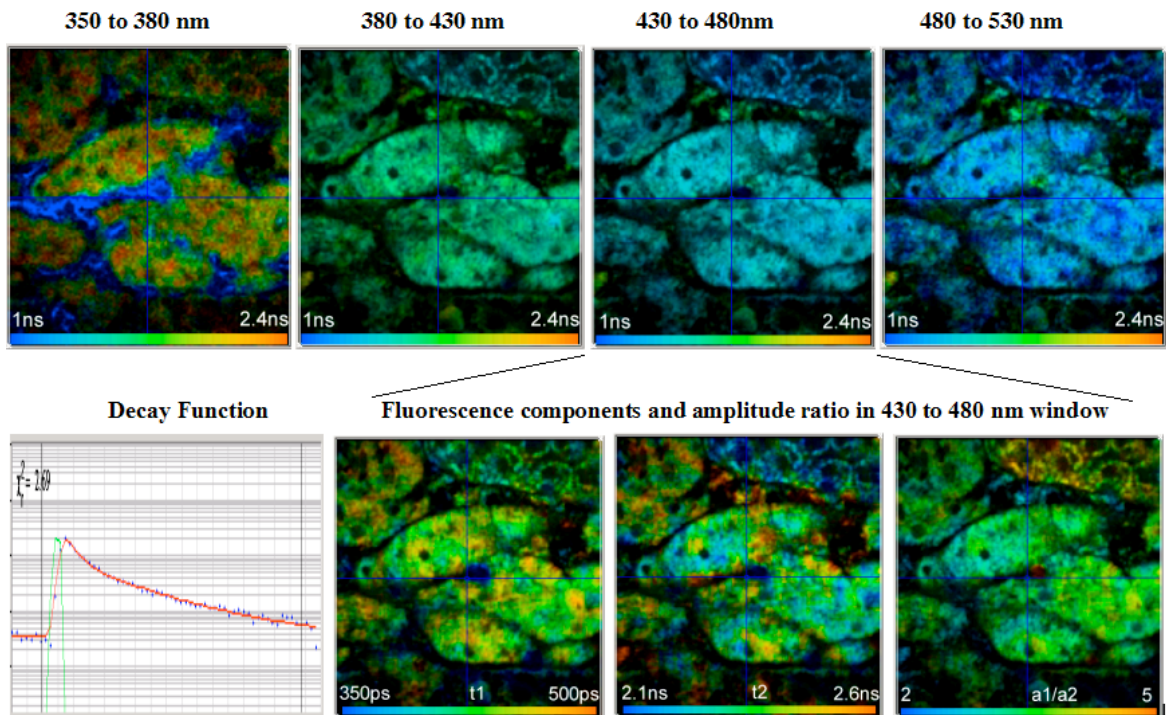


Fig. 37: Upper row: Single-exponential lifetime images in selected wavelength intervals. Lower row, left to right: Fluorescence decay curve at cursor position of 430 to 480 nm image with double exponential fit (red), lifetime image of the fast decay component, lifetime image of the slow decay component, image of the amplitudes of the lifetime components.

Troubleshooting

If the PML / SPC system does not work as expected please check the following details:

All count rates are present, but no curves or not all curves are displayed

Check that 'Points X' is set to '16' and that you have set a reasonable 'Delay' in the page control section of the System Parameters. In the 'Single' or 'Oscilloscope' mode, check the 2D Trace parameters. Make sure that the correct 'curves' are displayed, and that the 'Page' is the same as 'Measured Page' in the main panel. Please see Fig. 8.

No CFD count rate

Check the DCC settings. The +12V, +5V, and -5V buttons must be enabled, and the outputs must be enabled (see Fig. 12). Please note that, for safety reasons, the DCC-100 starts with all outputs disabled. Make sure that a reasonable gain is set. Single photon detection requires a gain above 80%, correct operation typically 90 to 95%. Make sure that the 15 pin power supply cable is connected to the upper or lower connector of the DCC-100 and that you control the DCC parameters of the right connector. Make sure that the 50-Ω SMA cable is connected from the PML output to the CFD input.

Large differences in channel efficiency, large crosstalk between channels

Increase DCC gain or decrease CFD threshold. Make sure that 'Delay' in the page control section of the System Parameters is set correctly. Check your system for electrical noise. Disconnect a network cable possibly connected to the computer.

CFD rate present, but no ADC rate

Make sure that the SYNC signal is present at the Sync input of the SPC card. The SYNC rate should correspond to the repetition rate of the light source used. Make sure that the 15 pin routing cable is connected to the routing connector of the SPC card. Some SPC cards have two connectors; the right connector is the one closer to the computer motherboard.

CFD rate present, but ADC rate very low. Only random photons detected.

The signal is outside the recorded time range. This happens especially for low-repetition rate signals. Usually the delay in the SYNC channels is too small. It may then happen that a time interval shortly before the laser pulse is recorded. See [3]; the SYNC pulse should arrive some 10 ns *after* the photon pulses. Make sure that the light arrives at the detector. If you have optical fibres feeding the light into a PML-SPEC assembly, check that the fibres are not broken and correctly connected. Make sure that the fibre is really an optical fibre and not an electrical SMA cable.

Another detector connected to the SPC module refuses to work

Disconnect the routing cable from the SPC module. When the PML is inactive it delivers a 'disable count' signal.

Poor time resolution, poor shape of IRF

Check your system for electrical noise. Disconnect a network cable possibly connected to the computer. Check for optical effects, such as photon migration in a scattering solution, and optical reflections.

Signals are detected even for DCC gain = 0

Check the CFD threshold. It should be between -50 mV and -100 mV. Check your system for electrical noise. Disconnect a network cable that is possibly connected to the computer.

Assistance through bh

Software updates, new handbook versions and application notes are available from the bh web site, www.becker-hickl.de. Furthermore, we are pleased to support you in all problems concerning the measurement of fast electrical or optical signals. This includes discussions of new applications, the installation of the SPC modules, their application to your measurement problem, the technical environment and physical problems related to time-resolved spectroscopy. Simply call us or send us an email.

Should there be a problem with your PML or SPC module, please contact us. To fix the problem we ask you to send us a data file (.sdt) of the questionable measurement or, if a measurement is not possible, a setup file (.set) with your system settings. Furthermore, please add as much as possible of the following information:

Description of the Problem

SPC and PML Module, Type and Serial Number

Software Version

Detector type, PMT Cathode type

DCC-100 settings

Laser System: Type, Repetition Rate, Wavelength, Power

SYNC Signal Generation: Photodiode, Amplitude, Rise Time

Optical System: Basic Setup, Sample, Monochromator

System Connections: Cable Lengths, Ground Connections. Add a drawing if necessary.

Environment: Possible Noise Sources

Your personal data: E-mail, Telephone Number, Postal Address

The fastest way is to send us an email with the data file(s) attached. We will check your system settings and – if necessary – reproduce your problem in our lab. We will send you an answer within one or two days.

Becker & Hickl GmbH

Nahmitzer Damm 30

12277 Berlin

Tel. +49 / 30 / 787 56 32

FAX +49 / 30 / 787 57 34

<http://www.becker-hickl.de>

email: info@becker-hickl.de

Specification

Electrical

Number of Channels	16
Arrangement	linear (1 by 16)
Active Area (each channel)	0.8 × 16 mm
Channel Pitch	1 mm
Spectral response	300 to 650 nm (bialkali) 185 to 650 nm (bialkali, UV window) 300 to 820 nm (multialkali)
Dark count rate (total, 22°C, typical values)	Bialkali 100 counts per second Multialkali 1000 counts per second
Timing Output Polarity	negative
Average Timing Pulse Amplitude	50 to 100 mV at -900V
Time Resolution (FWHM of IRF)	150 ps (typical value, for individual channels)
Time Skew between Channels	< 100 ps
Timing Output Connector	SMA, 50Ω
Misrouted Photons (100 kHz Count Rate)	< 0.1 %
Suppressed Photons (100 kHz Count Rate)	< 1 %
Routing Signal	4 'Channel' bits + 'Disable Count' bit, TTL/CMOS
Optimum 'Latch Delay' in SPC module	0 ns (SPC-630, 730, 830) 20 ns (SPC-140)
Connector for routing and power supply	15 pin Sub-D / HD (3 rows of pins)
Power Supply	+5V, -5V, +12V, from DCC-100 card
Gain control signal	0 to 1V, from DCC-100 card
Overload shutdown	at >2μA channel current, via DCC-100 card
Dimensions	50 mm × 50 mm × 168 mm

15 Pin Sub-D HD connector Pin assignment

1	+5 V
2	Routing, /R0 (TTL)
3	Routing, /R1 (TTL)
4	Routing, /R2 (TTL)
5	GND
6	-5 V
7	Routing, /R3 (TTL)
8	do not connect
9	do not connect
10	+12 V
11	do not connect
12	/Overload (TTL, open collector)
13	Gain Control, 0 to 1 V
14	/Disable Count (TTL)
15	GND

Mechanical

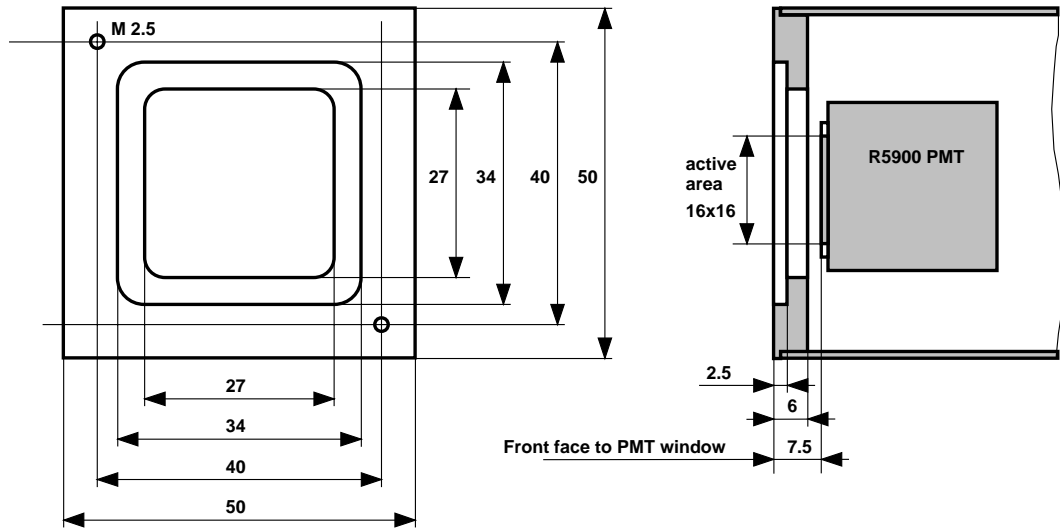


Fig. 38: Front end, outline in millimeters

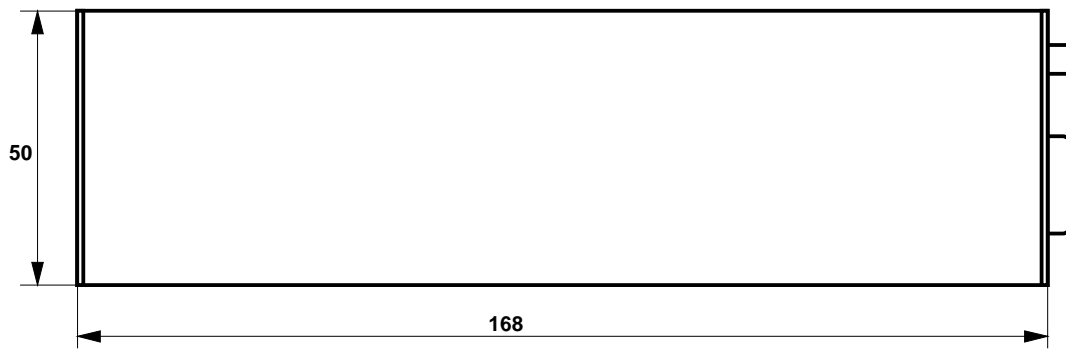


Fig. 39: Side View, outline in millimeters

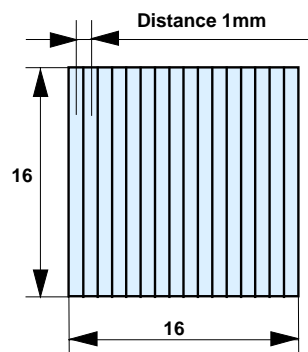


Fig. 40: Active area of photocathode, outline in millimeters

References

1. A. Bassi, J. Swartling, C. D'Andrea, A. Pifferi, A. Torricelli, R. Cubeddu, Time-resolved spectrophotometer for turbid media based on supercontinuum generation in a photonic crystal fibre, *Opt. Lett.* 29, 2405-2407 (2004)
2. W. Becker, *Advanced time-correlated single-photon counting techniques*. Springer, Berlin, Heidelberg, New York, 2005
3. W. Becker, *The bh TCSPC Handbook*, Becker & Hickl GmbH, available on www.becker-hickl.com (2005)
4. W. Becker, A. Bergmann, C. Biskup, D. Schweitzer, M. Hammer, Time- and Wavelength-Resolved Autofluorescence Detection by Multi-Dimensional TCSPC, *Proc. SPIE* 5862, 174-181 (2005)
5. W. Becker, A. Bergmann, M.A. Hink, K. König, K. Benndorf, C. Biskup, Fluorescence lifetime imaging by time-correlated single photon counting, *Micr. Res. Techn.* 63, 58-66 (2004)
6. W. Becker, A. Bergmann, G. Biscotti, K. Koenig, I. Riemann, L. Kelbauskas, C. Biskup, High-speed FLIM data acquisition by time-correlated single photon counting, *Proc. SPIE* 5323, 27-35 (2004)
7. W. Becker, A. Bergmann, *Timing Stability of TCSPC Experiments*, Becker & Hickl GmbH (2004), available on www.becker-hickl.com
8. W. Becker, A. Bergmann, C. Biskup, T. Zimmer, N. Klöcker, K. Benndorf, Multi-wavelength TCSPC lifetime imaging, *Proc. SPIE* 4620 79-84 (2002)
9. W. Becker, A. Bergmann, H. Wabnitz, D. Grosenick, A. Liebert, High count rate multichannel TCSPC for optical tomography, *Proc. SPIE* 4431, 249-245 (2001)
10. W. Becker, *Verfahren und Vorrichtung zur Messung von Lichtsignalen mit zeitlicher und räumlicher Auflösung*, Patent DE 43 39 787 (1993)
11. W. Becker, A. Bergmann, *Detector assemblies for picosecond microscopy*, Becker & Hickl GmbH, www.becker-hickl.com
12. Becker & Hickl GmbH, DCC-100 detector control module, manual, www.becker-hickl.com
13. Becker & Hickl GmbH, 16 channel detector head for time-correlated single photon counting, manual, www.becker-hickl.com
14. Becker & Hickl GmbH, BDL-375, BDL-405, BDL-475 Ultraviolet and Blue Picosecond Diode Laser Modules, www.becker-hickl.com
15. A. Bergmann, *SPCImage Data Analysis Software for Fluorescence Lifetime Imaging Microscopy*, Becker & Hickl GmbH, available on www.becker-hickl.com
16. D.K. Bird, K.W. Eliceiri, C-H. Fan, J.G. White, Simultaneous two-photon spectral and lifetime fluorescence microscopy, *Appl. Opt.* 43, 5173-5182 (2004)
17. C. Biskup, L. Kelbauskas, Th. Zimmer, S. Dietrich, K. Benndorf, W. Becker, A. Bergmann, N. Klöcker, Spectrally resolved fluorescence lifetime and FRET measurements, *Proc. SPIE* 5700, 188-196 (2005)
18. W. Denk, J.H. Strickler, W.W.W. Webb, Two-photon laser scanning fluorescence microscopy, *Science* 248, 73-76 (1990)
19. M. Göppert-Mayer, Über Elementarakte mit zwei Quantensprüngen, *Ann. Phys.* 9, 273-294 (1931)
20. Hamamatsu Photonics K.K., R5900U-16 series Multianode photomultiplier tube (2001)
21. K. König, Multiphoton microscopy in life sciences, *J. Microsc.* 200, 83-104 (2000)
22. H. Kume (ed.), *Photomultiplier Tube*, Hamamatsu Photonics K.K. (1994)
23. J.R. Lakowicz, *Principles of Fluorescence Spectroscopy*, 2nd edn., Plenum Press, New York (1999)
24. A. Liebert, H. Wabnitz, D. Grosenick, R. Macdonald, Fiber dispersion in time domain measurements compromising the accuracy of determination of optical properties of strongly scattering media, *J. Biomed. Opt.* 8, 512-516 (2003)
25. K. Maxwell, G.N. Johnson, Chlorophyll fluorescence - a practical guide, *Journal of Experimental Botany* 51, 659-668 (2000)
26. D.V. O'Connor, D. Phillips, *Time-correlated single photon counting*, Academic Press, London (1984)
27. J. Pawley (ed.), *Handbook of biological confocal microscopy*, 2nd edn., Plenum Press, New York (1995)
28. A. Rück, F. Dolp, C. Hülshoff, C. Hauser, C. Scalfi-Happ, FLIM and SLIM for molecular imaging in PDT, *Proc. SPIE* 5700, 182-187 (2005)

Index

- Afterpulsing 22
- Amplitude jitter of photon pulses 15
- Assistance through bh 35
- Autofluorescence
 - FLIM measurement 32
 - Single-point measurement 30
- Background count rate 21
 - Afterpulsing 22
 - dark count rate 21
- BDL-405 diode laser 26, 30
- Bialkali cathode 20
- Blaze wavelength 24
- Block Diagram of PML-16C 4
- CFD 16
 - Threshold 17
 - Zero-cross level 17
- CFD parameters 9
- Channel register 5
- Channel Uniformity 19
 - Efficiency 19
 - Transit time 20
- Chlorophyll transients 30
- Confocal detection 26
- Connector
 - of DCC-100 7
 - of PML-16C 36
- Constant fraction triggering 16
- Dark count rate 21
- DCC-100 7, 12, 26, 30
 - Enable outputs 12
 - Gain control 12
 - Overload shutdown 13
 - Supply voltages of PML-16C 12
- Delay parameter 8
- Diode laser, ps 26, 30
- Disable Count Signal 5, 6
- Discriminator
 - Constant fraction 16
 - internal, of PML-16C 13
- Display parameters 9
 - f(txy) mode 10
 - Scan Sync In mode 11
- DOT 25
- Enable DCC-100 outputs 12
- f(txy) mode 10
- Fibre bundle 25, 27
- Fibre probe 30
- FLIM 11, 26
- f-number 24
- Gain control 7, 12
- Grating 24
- High voltage 7, 13
- Instrument response function 17, 18
- Internal threshold of PML-16C 13
- IRF of PML-16C 17, 18
- Laser scanning microscope 26
 - Confocal detection 26
 - Descanned detection 26
 - Non-descanned detection 27
 - Two-photon excitation 26
- Multialkali cathode 20
- Multianode PMT 5
- MW-FLIM 26
- NADH 33
- Non-descanned detection 27
- Oscilloscope mode 9
- Outline of PML-16C 37
- Overload shutdown 8, 13, 28
- Photocathode
 - dark counts 21
 - of PML-16, outline 37
 - spectral response 20
- Pin assignment, PML-16C 36
- Pinhole 26
- PML-16
 - Channel Uniformity 19
- PML-16C
 - applications 30
- PML-16C
 - block diagram 4
 - IRF 17
 - mechanical outline 37
 - single-electron response 15
 - specification 36
- PML-16C, pin assignment 36
- PML-SPEC 24
 - Blaze wavelength 24
 - Fibre coupling 25
 - f-number 24
 - Grating 24
 - Slit width 25
- PMT
 - Principle 14
 - SER 14
 - Single-electron response 14
- Polychromator 24
- Quantum efficiency 21
- R5900 5
- Routing Signal 5
- Safety 13
- Scan Sync In mode 11, 26
- Second harmonic generation 32
- SER 14
 - Amplitude distribution 15
 - Amplitude jitter 15
 - of PML-16C 15
- SHG in tissue 32
- Shutter 28
- Single mode 9
- Single-electron response 14
 - amplitude distribution 15
 - of PML-16C 15
- Single-mode fibre 26
- Single-photon detection 14
- Single-photon pulses 14
- Specification of PML-16C 36

Spectral response	20	Oscilloscope mode	9
Spectral sensitivity	21	Single mode	9
Status LEDs of PML-16C	8	Troubleshooting	34
System parameters of TCSPC card	8	Two-photon excitation	26
TCSPC system parameters	8	Descanned detection	26
Trace parameters	9	Non-descanned detection	27